Titanium Dioxide for Hydrogen Economy: a Brief Review

N.V. Chirkunova[1,2,*], N. Islavath[3], M.V. Dorogov[1]

[1] Institute of Advanced Data Transfer Systems, ITMO University, Kronverkskiy pr., 49, lit. A, 197101, Saint-Petersburg, Russia
[2] Institute of Advanced Technologies, Togliatti State University, Belorusskaya str. 14, 445667, Togliatti, Russia
[3] Analytical Sciences Division, CSIR - Indian Institute of Petroleum, P.O. Mohkampur, Dehradun, 248005, Uttarakhand, India

Article history	Abstract
	Our research is mainly focused on solving problems related to the production of hydrogen and its storage, as well as the creation of autonomous energy systems using renewable energy sources. Technological solutions for green energy depend on the development of new materials with desired properties that are able to reversibly accumulate hydrogen under appropriate environmental conditions (temperature, pressure) and on the technological processes allowing to obtain molecular hydrogen without significant energy consumption. The creation of materials with fundamentally new characteristics is inextricably linked with the production of nanoscale systems with properties that are controlled at the atomic and molecular level. The review considers the results of studies on the possibilities of using various nanostructures of titanium dioxide known for its catalytic properties and high stability in various applications of hydrogen energy. Much attention is paid to the promising direction of solid-state storage of hydrogen using hydride pastes and high-entropy alloys.

CONTENTS

1. INTRODUCTION

Fossil hydrocarbon fuels are the main source of energy today. Fossil energy sources are exhaustible resources, and their usage is one of the reasons for environmental pollution, which limits the possibility of using such energy resources in future. Non-renewable resources can be replaced by more affordable and environmentally friendly energy sources such as hydrogen (H_2), solar and wind energy. Solar and wind energy are not stable in power generation as they depend on time of day and location. Recently, hydrogen has gained attention as a sustainable alternative for generating and storing energy. It has an energy density higher than the most modern lithium-ion batteries [1–3]. In addition, hydrogen is the most common element in nature and a part of most organic and many inorganic compounds, which allows to obtain this fuel from various sources. Hydrogen has the advantage of a very high calorific power. The product of hydrogen combustion is water which does not cause any ecological damage unlike the combustion of hydrocarbons. The reaction of gaseous hydrogen with oxygen to form water provides

* Corresponding author: N.V. Chirkunova, e-mail: natchv@yandex.ru

a sufficient amount of energy in the form of heat or electric current. Gaseous hydrogen is of great interest as an environmentally friendly energy carrier. Therefore, methods of obtaining it in sufficient quantities for the needs of hydrogen energy are actively studied [2–10]. The main elements of the hydrogen economy include the production, delivery, storage, conversion and use of hydrogen. Hydrogen differs from other fuels in that it is difficult to store and transport. At present, compressed H_2 is the main method of H_2 storage on-board vehicles; and the pressure in the tanks varies from 35 to 70 MPa. High pressure H_2 tanks are limited in use because they are expensive and heavy, take up a lot of space and are difficult to integrate into small vehicles [11].

Researchers are therefore motivated to develop new materials that can replace compressed hydrogen tanks while facilitating the transition to hydrogen as an energy vector and accommodating new applications such as stationary and portable devices. The new materials, including high entropy alloys, sorbent materials and hydrides, show great potential for storing hydrogen in chemical or solid form and demonstrate excellent reversibility and kinetics. However, their inherent instability has been a limiting factor in their widespread adoption. In recent years, high entropy alloys, hydride paste technologies are emerged as a promising approach for producing high-purity hydrogen and offers the advantage of easy transportation and user-friendliness. It has a specific energy of 1900 W·h/kg, which is 9–10 times higher than that of lithium-ion batteries. Moreover, high entropy alloys/hydride paste provides higher energy density compared to 700-bar pressure tanks, making it suitable for various vehicles, including those used in remote locations.

Among various metal alloys, high-entropy alloys and power paste materials have shown potential as hydrogen storage materials. High-entropy hydrides (HEHs), such as magnesium hydrides, exhibit exceptional hydrogen storage abilities with hydrogen-to-metal ratios (H/M) of up to 2.5. These materials are composed of at least five principal elements, each with atomic percentages ranging from 5% to 35%. The unique composition of HEHs leads to the formation of single-phase solid solutions with crystal structures like body-centered cubic (BCC), face-centered cubic (FCC), hexagonal close-packed (HCP), and C14 Laves phase structures, which contribute to their remarkable hydrogen storage properties. Despite these advantages, hydride paste is characterized by rapid surface oxidation and H_2 migration, which reduces its energy density and stability [12].

The addition of semiconductor nanoparticles such as CuO, TiO_2, Ga_2O_3 is one of the promising ways to improve the properties of materials used in hydrogen production and storage devices. Nanoscale materials have many special properties that differ from the bulk properties of the same materials [13–18]. For example, titanium dioxide is a fairly cheap and widespread material known for its excellent photocatalytic properties [19–24]. Anodes based on titanium dioxide nanotubes or copper oxide nanowhiskers are a promising working catalyst in the process of hydrogen production by photoelectrochemical water decomposition [25–27]. Addition of nanocrystalline titanium dioxide supported on carbon reduces MgH_2 dehydrogenation operating temperatures.

This review describes methods for obtaining promising materials for the synthesis and storage of hydrogen, including special materials with nanostructured components. Such structures are obtained by various methods: electrochemical, chemical vapor deposition, microwave, solvothermal (including hydrothermal), sonochemical, sol-gel, etc. [13,28–30]. It is known that the properties (optical, magnetic and electronic, catalytic properties and reactivity change) of synthesized materials directly depend on the size, structural and morphological features, which are strongly influenced by the production methods [16,31–34]. While there are legions of the methods, this review presents a description of some widely used methods for obtaining titanium dioxide nanostructures.

2. NANOSIZED TITANIUM DIOXIDE AND METHODS OF ITS PRODUCTION

Titanium dioxide (TiO_2) is a chemically stable, non-toxic, biocompatible, inexpensive material with very high electrical constant and photocatalytic activity. Titanium dioxide is a wide-gap indirect junction *n*-type semiconductor. Natural titanium dioxide exists in the form of three minerals: rutile, anatase and brookite, which are polymorphic modifications (the band gap for anatase is 3.18 eV, for brookite is 3.27 eV, for rutile is 3.03 eV) [28]. Under laboratory conditions (for example, at high pressures and low temperatures), other modifications can be obtained. Overall, eleven polymorphic modifications of crystalline TiO_2 are reported in the literature; it can also be obtained in the amorphous state [35]. Rutile TiO_2 is the most stable form, while the anatase and brookite phases are metastable and can transform into the rutile phase when heated to a high temperature (~750 °C). Anatase and rutile TiO_2 are most often mentioned as photocatalysts. An increased photocatalytic activity of the mixed form of rutile and anatase TiO_2 has been reported [28]. The authors explain the improvement in the photocatalytic properties of the mixed form of TiO_2 by the fact that during the transfer of electrons from anatase to rutile in the low-energy region of electron capture, the rate of charge carrier recombination can decrease, and this fact also contributes to the efficient formation of catalytically "hot spots" in anatase TiO_2 [28,36]. The reports of photocatalytic performance of
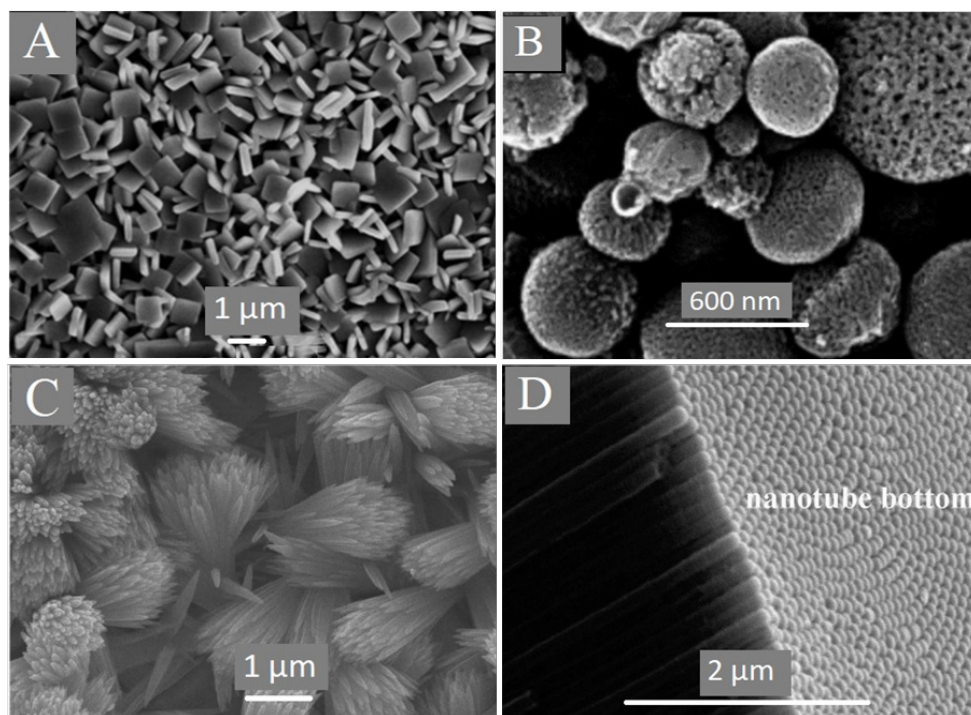
Fig. 1. SEM photographs of various nanostructures TiO₂: a) the anatase TiO₂ nanosheets. Reproduced with permission from Ref. [41], © 2009 American Chemical Society; b) the N-F-codoped TiO₂ spherical particles with a porous surface morphology. Reproduced with permission from Ref. [42], © 2005 American Chemical Society; c) the rutile TiO₂ nanoflowers. Adapted from Ref. [43]; d) SEM image of the freestanding TiO₂ nanotube arrays (side view). Reproduced with permission from Ref. [44], © 2008 American Chemical Society.

TiO₂ brookite began appearing only a few years ago due to difficulties with pure TiO₂ brookite preparation and its relatively low photoreactivity. However, heterophasic TiO₂ can effectively promote electron transfer from one crystal phase to another, which shows excellent photocatalytic performance. Various studies report excellent photocatalytic performance of biphasic TiO₂ such as anatase/rutile, anatase/brookite, rutile/brookite [37–39]. Titanium dioxide is chemically quite inert and its chemical activity begins to increase when heated, when it interacts with acids, bases, alkali metal halides, the metals themselves, hydrogen, coal, etc. The most active polymorphic modification is anatase, and the most inert is rutile.

TiO₂ nanocrystals have a number of advantages over bulk counterparts in terms of potential applications because of the high surface to volume ratio, charge transfer rate and lifetime, as well as the effective contribution to the separation of photogenerated holes and electrons [13,28,40]. In this regard, it is important to control the particle size, shape, and composition of the synthesized TiO₂. Researchers have obtained various TiO₂ nanostructures, such as nanoparticles, nanotubes, nanorods, nanofibers and nanoflowers with unique characteristics (Fig. 1).

These structures can be fabricated using a variety of methods: micelle and inverse micelle methods, hydrothermal method, sol-gel, solvothermal method, direct oxida-

tion method, sonochemical method, etc. Below we consider the methods which, in our opinion, are most often used to obtain titanium dioxide nanostructures for use in hydrogen production applications.

2.1. Electrochemical anodization

The method of electrochemical anodization at a constant voltage and different anodization time is used to obtain structures from titanium dioxide nanotubes. The anodization process consists in immersing a titanium foil in an electrolyte and connecting it to the positive pole of a direct current source. During the passage of electric current through the electrolyte, oxygen is released in active form on the anode, which interacts with titanium forming an anodic oxide film. The growth of the anode layer does not occur on the outer surface of the sample, but under the layer of the previously formed oxide film, that is, at the interface between titanium and the anode film. The orientation of nanotubes, the distance between the tubes, and the diameter depend on the used electrolyte, temperature, anodization mode, and other parameters. Various substances are used as electrolytes such as aqueous solutions of fluorine-containing acids (hydrofluoric, phosphoric and sulfuric with a fluorine-containing component), organic electrolytes based on ethylene glycol, glycerin, their complex compositions with the addition

of hydrofluoric acid or other fluorine compounds (for example, NH$_4$F), etc. [45].

Titanium dioxide nanotubes are of great research interest because of their functional properties, such as, for example, a large surface area. Nanotubes have wide technological applications in the field of photocatalysis, photoelectrochemical hydrogen production, gas sensors, etc. Titanium dioxide nanotube arrays have significant superior properties such as charge transfer and efficient separation of electron-hole pairs which are effectively used in photoelectrochemical cells with water splitting for hydrogen production [28,45–47].

2.2. Solvo- and hydrothermal method

The hydro/solvothermal method is based on reactions taking place in closed systems at high pressure and temperature. During the synthesis, precursors, solvents, and surfactants containing functional groups are mixed. Further heating is carried out in a special reaction vessel called an autoclave. The solvothermal method is very similar to the hydrothermal method, the difference lies in the use of a non-aqueous solvent and higher process temperatures. This is due to the fact that some organic solvents have high boiling points. The choice of synthesis conditions (the initial pH value of the medium, the duration and temperature of the synthesis, and the pressure in the system) and the type of surfactant make it possible to purposefully obtain nanomaterials of various sizes, shapes, and crystalline phases. A significant expansion of the possibilities of the hydrothermal method is facilitated by the use of additional external influences on the reaction medium in the course of synthesis. At present, a similar approach has been implemented in hydrothermal-microwave, hydrothermal-ultrasonic, hydrothermal-electrochemical, and hydrothermal-mechanochemical synthesis methods. These processes have made the hydrothermal technique more attractive to ceramists and chemists due to improved kinetics. The duration of experiments is reduced by at least two orders of magnitude, which makes the technique more economical [28,48].

The hydrothermal method provides good control over the growth of TiO$_2$ crystal structures. A necessary condition for its preparation is the presence in the solution of some surface-active substances (surfactants), which actively influence the morphological evolution of oxide compounds in hydrothermal solutions. The agglomeration of nanoparticles can be controlled by careful selection of the ratio of starting materials, pH, time and temperature. The influence of solvents on the crystalline phase and the morphology of TiO$_2$ nanostructures has been extensively studied. An alkaline medium is used as a solvent, NaOH is considered the most popular solvent.

The solvothermal method makes it possible to obtain TiO$_2$ nanoparticles with a narrow size distribution and fineness. TiO$_2$ nanoparticles and nanorods were synthesized by the solvothermal method with and without the use of surfactants [49–51].

2.3. Sol-gel

The sol-gel method can be used to obtain nanoparticles, porous structures, fiber and bulk structures. The process of obtaining titanium dioxide using this technology consists of two stages: hydrolysis of titanium alkoxide (I) and polycondensation (II), with further isolation of water and alcohol as reaction products [40]. When carrying out the synthesis by this method, it is necessary to control the sol-gel process by varying its parameters. The concentration of the titanium-containing precursor greatly affects the crystallization process. In addition, the size, stability and morphology of the resulting sol is highly dependent on the molar ratio of water and titanium-containing precursor. Another parameter affecting the morphology of the final titanium dioxide powder is the pH of the prepared solution. The sol-gel method makes it easy to control the structural properties and particle sizes of titanium dioxide by changing the appropriate process conditions (pH, time, complexing agent, etc.) [14,52–59].

2.4. Chemical vapor deposition

Chemical vapor deposition (CVD) is widely used for obtaining thin films of TiO$_2$. TiO$_2$ particles are formed due to chemical reactions (e.g., hydrolysis of titanium alcoholates) occurring either in a gas mixture or on the substrate surface. The gas phase of TiO$_2$ can also be obtained by physical action, for example, by heating the titanium dioxide surface with an electron beam (electron beam deposition method). The source of electrons is a tungsten filament heated by electric current. The product does not contain any undesirable impurities typical of chemical methods, it is possible to obtain thick crystalline films with a grain size of less than 30 nm and a particle size of less than 10 nm [13,28,60,61].

When choosing a synthesis method, important criteria are the simplicity of the device, not too long duration, economy and safety of the process. From this point of view, the methods of synthesis and some properties of titanium dioxide were considered, the knowledge and understanding of which is necessary to obtain nanoparticles/nanostructures with desired properties. Different methods of synthesizing the same material can lead to materials that differ in chemical composition, crystallinity, and microstructure due to differences in the kinetics of the processes. The synthesis method is selected depending on
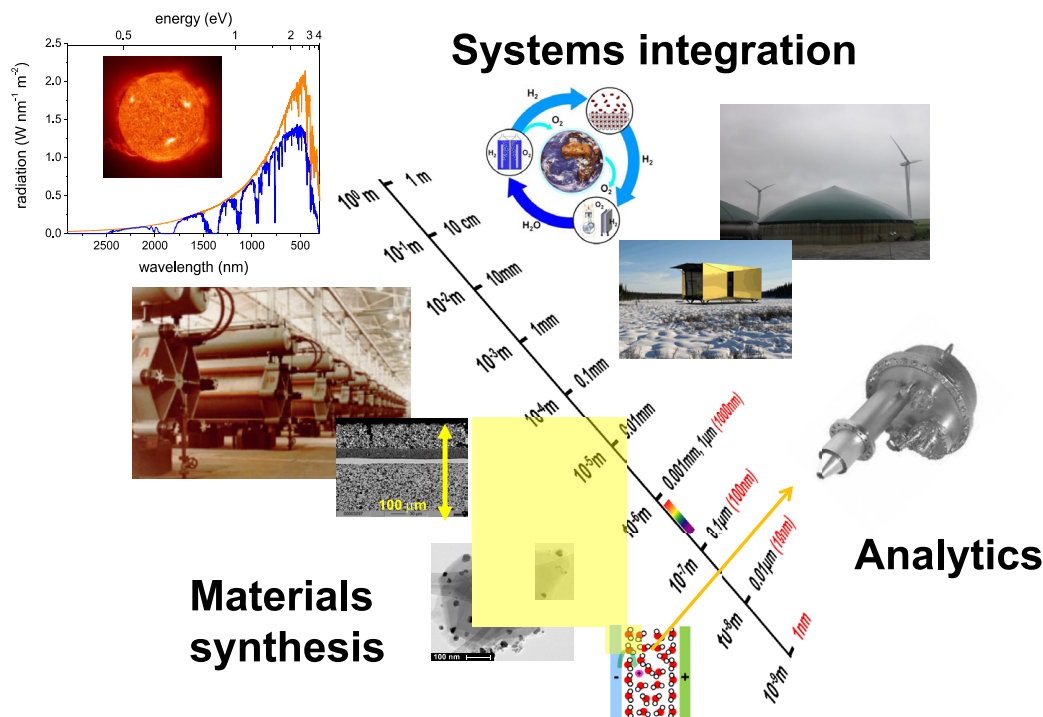
Fig. 2. The three hydrogen grand challenges in a nutshell: although at the beginning, the (atomistic) phenomena as characterized by state-of-the art analytics (challenge 1) are utilized by advance materials (challenge 2) which are part of big systems (challenge 3) to store and distribute the energy of the sun. The hydrogen grand challenge comprises research and development from the nano-scale to the macroscopic world. Reprinted under a Creative Commons Attribution License (CC BY) from Ref. [7], © 2016 Borgschulte.

the final characteristics of the resulting nanostructured material. For example, to obtain nanotubes, nanopores, and nanorods, the most commonly used methods are solvo- and hydrothermal synthesis, sol-gel, and electrochemical anodization. To obtain pure and highly structured films with a particle size of less than 10 nm, the chemical vapor deposition method is very convenient. Solvothermal and sol-gel methods make it possible to obtain various nanostructures with high dispersity and unique morphology (nanoflowers, urchinlike, nanosheets with dominant facets, etc.) Various combinations of these methods are widely used, including for improving the physicochemical properties of materials required for specific applications (doping of photocatalysts, sorbents, nanostructured composite materials for electrodes of photo- and electrochemical cells, etc.)

It follows from the review of literature data that the targeted synthesis of titanium dioxide nanostructures with desired properties is an urgent task for creating new generation materials capable of solving the most complex problems of our time, such as the transition to green energy.

3. OBTAINING HYDROGEN

Hydrogen in molecular form can be obtained from many resources such as fossil fuels, biomass and water [62]. Today, the main hydrogen production technologies can be classified depending on the raw materials used: fossil fuels or renewable resources (solar, wind, water, etc.). Fossil fuel-driven hydrogen technologies are the main sources of molecular hydrogen at this stage of the hydrogen energy industry, as production costs are highly correlated with fuel prices, which are still sustained. The main methods for producing hydrogen are hydrocarbon reforming (steam reforming) and pyrolysis [4,63,64]. After production, H_2 is placed in pressure storage tanks for transport. Compressed H_2 is not a user-friendly accumulator and must be transported to the place of use (for example, to a gas station) by a special trailer. Special care is also needed for the storage of hydrogen, as it is highly flammable and also easily oxidized in storage tanks and pipelines (Fig. 2).

However, the production of hydrogen fuel also requires energy costs. Another major disadvantage is the presence of carbon by-products. There is a classification of hydrogen production according to their environmental friendliness. Depending on production methods, hydrogen can be brown, grey, blue or green — and sometimes even pink, yellow or turquoise — although naming conventions can vary across countries and over time. Hydrogen produced by coal gasification is called brown hydrogen. The production of hydrogen from natural gas is called gray due to the fact that carbon waste is emitted. Hydrogen produced by a manufacturing process that uses carbon capture

and storage for the greenhouse gases produced when gray hydrogen is created is referred to as blue hydrogen. Hydrogen obtained by methane pyrolysis is turquoise. The production of hydrogen fuel using renewable energy is called green. For example, the electrolysis of water used to produce long-term energy storage of hydrogen requires a lot of energy. This energy can be obtained from renewable energy sources [65].

3.1. Steam methane reforming and coal gasification

Hydrogen for industrial and commercial use is produced by steam reforming of natural gas (reforming). It is a mature technology widely used in the oil refining industry. There are significant opportunities to develop new technologies that can reduce the cost of producing hydrogen from natural gas. Another fossil fuel—coal—can also be an energy source for hydrogen production. Therefore, today there is a significant production of hydrogen due to coal gasification and subsequent gas processing. Moreover, coal-derived gas can be converted to methanol for use both as an intermediate in the chemical industry and as a hydrogen carrier for subsequent reforming. The development of hydrogen production technology with a low carbon footprint remains an important challenge today. Carbon dioxide produced during hydrogen production is removed using capture and sequestration technology. To reduce costs, it is necessary to develop new and advanced technologies in all stages of the hydrogen gasification/production and separation process, which are currently developed. For example, by using pressure swing adsorption (PSA) technology in methane shifting and coal gasification to produce additional hydrogen and convert carbon monoxide to carbon dioxide, hydrogen is separated from the gas stream, and the residual gas from this separation can be recycled or burned [6].

Recent research has focused on increasing hydrogen production by direct thermal catalytic decomposition of methane to form elemental carbon and hydrogen as an attractive alternative to the traditional steam reforming process [66]. Various metals have been investigated as a catalyst for the decomposition of methane (Ni, Fe, Cu, Pd, Co, Pt, W, and others). These catalysts are often used in conjunction with support structures such as silica, magnesium, zirconium, titanium and carbon structures to increase the overall surface area of the catalyst. It is important to provide a large area for functioning as catalytic active sites during the reaction. The most attractive catalysts are catalysts based on nickel, ruthenium and platinum. These materials exhibit the highest activity and catalytic efficiency in the production of hydrogen in the process of thermal catalytic decomposition of methane [67]. However, their main disadvantage is rapid deactivation at high temperatures. Other supports such as TiO_2, MgO, ZrO_2 and Al_2O_3 give relatively lower carbon yields. To obtain highly concentrated hydrogen from the decomposition of methane, a higher conversion of methane in one pass is desirable [66].

3.2. Water electrolysis

One of the well-known methods for producing hydrogen is water electrolysis. However, the large-scale application of electrolyzes for renewable hydrogen production is hindered by a small number of active and stable electrocatalysts, as well as low energy conversion efficiency associated with the slow release of anodic oxygen and cathodic hydrogen [9]. In addition, the electrolysis of water produces O_2 and H_2 at the same time, which promotes the formation of reactive oxygen species, which creates an explosion hazard and, of course, destroys the membrane, shortening the life of the electrolyzer [2]. To increase the efficiency of the process, various electrocatalysts are used. Pt-based metals and alloys are the reference electrocatalysts for water electrolysis, but high cost and low durability severely limit their practical application. Electrolysis technologies are classified according to the type of electrolyte used and operating temperature: alkaline liquids, polymer membranes, solid oxide ceramics [68].

The principles of operation of the three main types of electrolysis technologies are shown in Fig. 3. The overall reaction is $H_2O \rightarrow H_2 + \frac{1}{2}O_2$. Oxygen evolution occurs at the anode, hydrogen evolves at the cathode. The case of solid oxide electrolysis shown is that of an O^{2-} conducting electrolyte, with a nickel/yttria-stabilized zirconia cathode and a lanthanum strontium manganite (LSM) anode.

Solid oxide electrolyzers usually operate at a fairly high temperature of 500–1000 °C with water in the form of steam. The solid oxide electrolysis process uses O^{2-} conductors, which are primarily made of nickel/yttrium stabilized zirconia. For the electrolysis of water in liquid alkaline media, an aqueous solution of KOH/NaOH is used as an electrolyte and operating temperatures are below 100 °C. An asbestos diaphragm and relatively inexpensive nickel materials are used as electrodes. The production of hydrogen by electrolysis of alkaline water is a simple, well-established technology. On the other hand, there are also disadvantages: limited current densities (below 400 mA/cm^2), low operating pressure and low energy efficiency. Polymer electrolyte membrane electrolyzers or proton exchange membrane electrolyzers operate in the low temperature range (typically below 100 °C). A proton exchange membrane, a perfluorosulfonic acid polymer (also known as Nafion^{TM}) is used as the electrolyte.

To date, the commercial introduction of polymer electrolytic membrane fuel cells requires overcoming two problems: low durability and high cost of membrane materials and platinum catalyst. The cost of Nafion^{TM} N117-
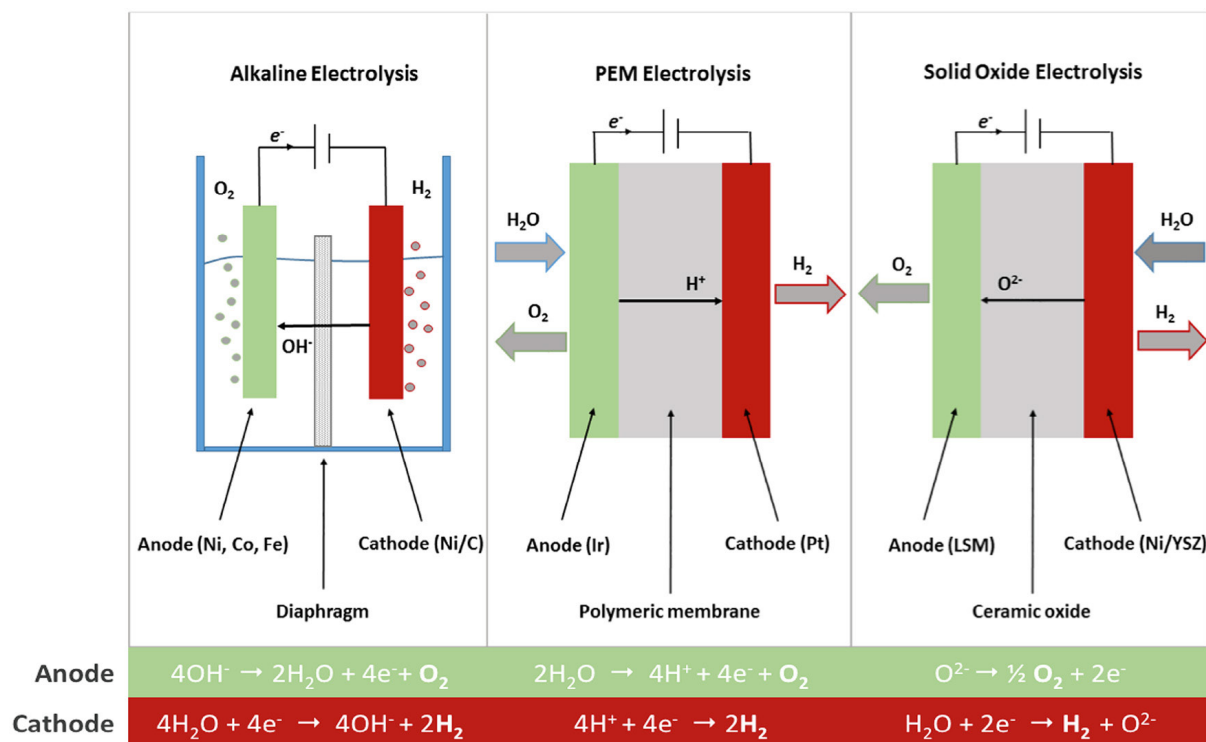
Fig. 3. Operation principles of alkaline, PEM (proton-exchange membrane) and solid oxide water electrolysis. Reprinted under a Creative Commons Attribution-NonCommercial-No Derivatives License (CC BY-NC-ND) from Ref. [69], © 2016 The Authors. Published by Elsevier Ltd.

type polymer electrolytic membranes used in automotive fuel cells is quite high and amounts to about 30% of the car's sales price [70]. Research continues in the direction of improving the performance properties, as well as reducing the cost of films such as Nafion. According to the literature data, when optimizing existing and creating new polymer electrolytes, it is necessary to ensure the resistance of materials to aqueous solutions of acids, as well as to control the water content necessary for proton conductivity. In addition, it is required to limit the swelling of polymeric materials in order to increase their mechanical stability [70–72].

The efficiency and stability of electrocatalytic materials is increased either by doping with transition metals (Fe, Co, Cr, V, Mn, etc.) or by reducing the loading of expensive catalysts (Ir) through the use of carriers with a large surface area (such as TiO_2, TiC, TaC) with the introduction of a catalytic phase into them [69,73]. Alternative materials such as perovskites, nanostructured materials are also used [46,74–76]. For example, an efficient cobalt-doped TiO_2 nanorod arrays electrocatalyst with a large number of oxygen vacancies and increased surface hydrophilicity has been proposed. This unique structure provides the electrocatalyst with highly efficient and stable electrocatalytic performance even at high current densities in alkaline electrolytes [77]. And as an alternative to commercial asbestos, TiO_2 composite membranes can be used in alkaline water electrolysis [68].

3.3. Photoelectrochemical splitting of water

One method that has been widely studied is the production of hydrogen from water using photoelectrochemical (PEC) processes. The photoelectrochemical process of water splitting occurs under the action of light when a semiconductor photoelectrode and an auxiliary counter electrode are immersed in an aqueous electrolyte. The first proposed photoanode consisted of titanium dioxide, and the counter electrode of platinum [78]. In the surface layer of the photoanode, when illuminated by photons with an energy exceeding the band gap of the semiconductor, electron-hole pairs are generated. For an *n*-type semiconductor, hydrogen is released due to the reduction of water by photoanode electrons that have passed through the external circuit to the counter electrode, while holes oxidize water to oxygen on the photoanode surface. Figure 4a shows a schematic diagram of a photoelectrochemical cell for water splitting, and Figure 4b shows a model of a photoelectrochemical process for water splitting using a metal-semiconductor composite (for example, Pt/TiO_2) instead of two electrodes connected by an electrical circuit. The metal-semiconductor composite structure is easily scalable for macro-sized PEC cells, especially in the form of nanopowder or nanostructures. Here, the metal component is usually referred to as the "cocatalyst" and the semiconductor as the "photocatalyst" [79]. Semiconductors with high activity and stability under solar irradiation include
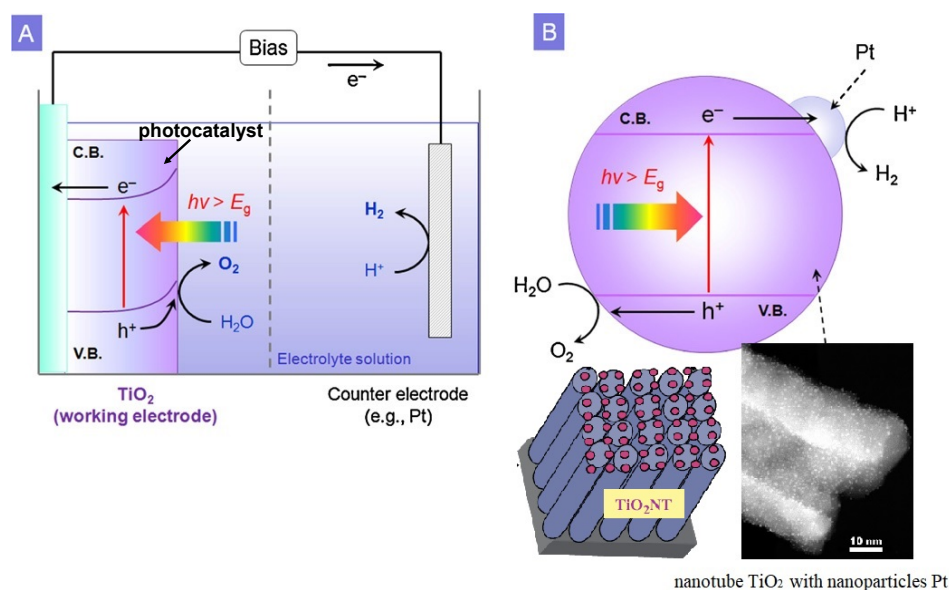
Fig. 4. a) A model of a photoelectrochemical water splitting process using a TiO_2 anode. Adapted from Ref. [79]. b) A model of a photoelectrochemical water splitting process using a metal-semiconductor composite (Pt/TiO_2). Adapted from Refs. [79,81,82].

TiO_2, WO_3, CdS, Ga_2O_3. The most common electrolytes are water solutions of sulfuric acid, phosphoric acid, sodium hydroxide and others [80].

An optimal semiconductor should have suitable energy band edge positions (semiconductor band gap) to absorb visible light and convert it into chemical energy. However, most basic semiconductors are active in ultraviolet light, which is only a small fraction (4%) of solar radiation. For example, TiO_2 has a band gap of 3.2 eV, which limits its activity in visible light. Therefore, it must be modified by doping with metal/non-metal ions (composites with metal and semiconductor nanoparticles) or used together with a cocatalyst to increase its activity in sunlight due to better charge separation. Usually noble metals are used as cocatalysts, but less expensive materials such as CdS, Cu_2O, NiO and perovskites can also be loaded [83].

Electrochemical cells consist of two electrodes immersed in an electrolyte. During cell operation, oxidation and reduction processes occur on each of the electrodes. The electrode at which reduction occurs is called the cathode, and the anode is the electrode at which oxidation occurs. In photoelectrochemical cells, processes occur when exposed to light. Further, the possibilities of using titanium dioxide as part of the anode and cathode electrodes of a photoelectrochemical cell are considered.

3.3.1. Photoanodes based on titanium dioxide

Titanium dioxide anode nanotubes (TNT) as an electrode have shown advantages because of their flexibility, economy and efficiency. The TiO_2 photoanode was the first known metal oxide in a photoelectrochemical water

splitting cell [78]. TNT TiO_2 anode nanotube films are a one-dimensional structure fabricated on a conductive and flexible titanium metal substrate.

Various strategies to improve the optical or electrical conductivity of the TiO_2-based electrode are used to enhance the performance of the photocell. For example, Ref. [84] reports on a method for disordering the upper TiO_2 nanolayer by hydrogenation in an H_2 atmosphere at a pressure of 20 bar at a temperature of about 200 °C for 5 days. The onset of optical absorption of the black hydrogenated TiO_2 nanocrystals was reduced to about 1.0 eV. This material got its name for its color, which is really black. The resulting black hydrogenated TiO_2 shows a breakthrough in expanding the solar absorption spectrum from 380 to 1200 nm. In addition, Hahn et al. [85] reported the high photoactivity of nanotubes with a high content of TiO_xC_y. TiO_2 nanotube films were treated by carbon-thermal reduction with acetylene and heating to 850 °C. These TiO_xC_y nanotubes can be used, for example, as an inert electrode with significant overvoltage for O_2 evolution, or as a highly efficient substrate for electrocatalytic reactions, for example, in methanol-based fuel cells.

3.3.2. The use of titanium dioxide in the production of cathodes

The metal oxide catalysts used in the cathodic hydrogen evolution reaction are not stable enough for efficient operation of the water splitting photoelectrochemical reaction cell. The problem of photocathode stability is related to the fact that the catalyst operates in an environment with the formation of atomic H^+ and the evolution of gaseous H_2. Majority of the studied photocathodes in the reaction

photoelectrochemical water splitting cell are *p*-type semiconductors, such as Cu_2O and CdS. Designs of cathodes with a passivating layer have been proposed to protect the semiconductor catalyst from attack by the resulting H^+ ions [86]. The *n*-type semiconductor titanium dioxide is used as a passivating layer because of its high corrosion resistance in alkaline media. However, the passivation layer increases the overvoltage and suppresses the exchange of electrons between the (photo)cathode and the electrolyte. To eliminate this effect, cocatalysts of noble metals and their oxides are used. Thus, the cathode of a photoelectrochemical reaction cell has a complex composite structure of a *p*-type semiconductor, one or two passivating layers of an *n*-type semiconductor, and a metal/metal oxide cocatalyst [87].

Recently, a highly active and stable photocathode for the reaction of hydrogen evolution has been presented [88]. It exhibits self-improving performance after a five-stage cathodic reduction process. Work [88] demonstrates a feasible strategy for forming a multi-junction composite for an efficient hydrogen evolution reaction in a photoelectrochemical water splitting cell with a titanium dioxide nanotube cathode.

An analysis of hydrogen production technologies has shown that titanium dioxide is widely used in these technologies. In one case, TiO_2 acts as a reaction catalyst, cocatalyst or catalyst support (thermal catalytic decomposition of methane, water electrolysis). In another case, it is used in the material of electrodes (water electrolysis, photoelectrochemical splitting of water). In both cases, interest in titanium dioxide is due to its bulk properties, such as high corrosion resistance, high mechanical strength, biocompatibility and its properties in the nanostructured state: efficient charge transfer and separation of electron-hole pairs, high surface activity. In the technology of hydrogen production by photoelectrochemical water splitting, titanium dioxide is the most frequently mentioned electrode material. This is also connected with the pioneering work of A. Fujishima and K. Honda [78] on the photocatalytic splitting of water in 1972, which caused a wave of research work aimed at studying the photocatalytic properties of titanium dioxide and other semiconductors. Thus, it is with fairly simple and affordable methods for obtaining titanium dioxide nanostructures (nanotubes, nanopores, nanoflowers, nanoparticles down to several nanometers), which allow to improve the photocatalytic process.

4. HYDROGEN STORAGE

Hydrogen storage is a critical challenge in transitioning to a hydrogen-based economy, primarily due to its low volumetric energy density and difficulties in handling and transporting hydrogen safely. Various approaches to hydrogen storage include high pressure compressed gas, liquid hydrogen cryogenic storage, solid state storage, and electrochemical storage [89]. Solid storage of hydrogen is easy to implement in materials such as metal hydrides, complex hydrides, carbonaceous materials, as well as activated carbon, graphene, and carbon nanotubes [90,91]. Solid-state hydrogen storage systems have emerged as a promising solution, offering high volumetric energy density, safety, and reversible hydrogen absorption/desorption capabilities over multiple cycles. Extensive investigations have been carried out on intermetallic compounds for H_2 storage, with the International Energy Society (IES) setting targets for gravimetric doping levels of 7–8 wt.% and volumetric concentrations of 70 g/l. In the pursuit of solid-state H_2 storage, the IES has explored a range of materials, including chemical hydrides, sorbents, complex hydrides, and conventional hydrides.

Figure 5 shows the concept of generating hydrogen using the PowerPaste (a) and the high-entropy alloy for hydrogen storage (b).

Solid-state hydrogen storage offers several advantages, including reduced transportation risks and the ability to store hydrogen in residential settings. This alternative approach is gaining attention, particularly in the hydrogen transportation sector, where traditional high-compressed hydrogen tanks may be impractical for smaller vehicles like motorcycles or scooters. The use of portable hydrogen generators based on power paste or high-entropy alloy materials provides a more compact and efficient solution for hydrogen storage and transportation, eliminating the need for high-compressed tanks. These advancements in solid-state hydrogen storage have the potential to make hydrogen as a fuel more accessible and practical for a wide range of applications, including small vehicles.

4.1. Sorbents

Hydrogen molecules can be reversibly stored on materials with a large surface area due to weak physisorption forces between gas molecules and solids. Sorbents such as metal-organic frameworks (MOFs), carbon-based materials including carbon nanotubes (CNTs) and graphene, and boron nitride (BN) possess advantageous properties such as low density, high surface area, and excellent reversibility and kinetics [94–98]. However, to achieve economic feasibility in practical applications, a favorable H_2/sorbent energy in the range of 4.6–6.9 kcal/mol is required. This method has many advantages: high storage density, excellent reversibility, as well as high charge-discharge rate and cyclic stability. However, the disadvantage is that low temperatures (–196 °C) and high pressure are required for
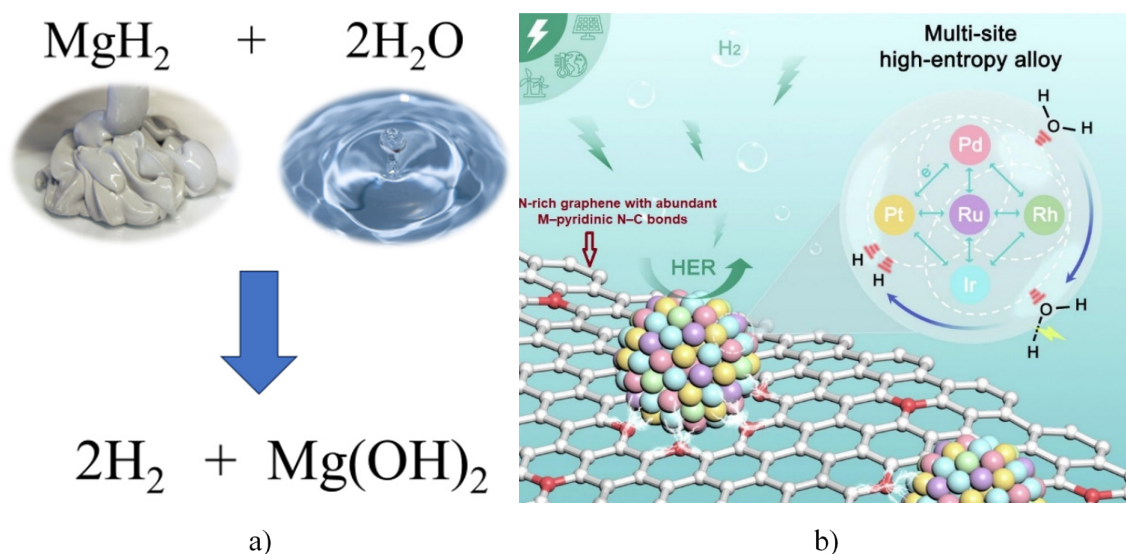
Fig. 5. a) Power paster. Adapted from Ref. [92]. b) High entropy alloy for hydrogen storage. Adapted from Ref. [93].

significant adsorption [99]. On the other hand, desorption requires high temperatures due to the lack of hydrogen adsorption-desorption reversibility due to its strong binding strength and slow kinetics.

Among the most interesting options for creating high-capacity (up to 6–7 wt.%) hydrogen sorbents are nanotubes and fullerenes with Ti atoms on the surface (to which hydrogen is attached), systems of graphene layers with nanotubes between them (with the addition of Li) [100,101]. However, transition metal atoms can cluster on the surface of nanotubes or fullerenes, as this is energetically favorable, and this can reduce hydrogen sorption [102]. S. Rouzbeh et al. [103] developed porous three-dimensional pillared BN nanostructures (3DPBN) with an impressive surface area exceeding 2200 m^2/g and explored their potential for H_2 storage. The results demonstrated a maximum H_2 uptake of 8.65 wt.% at 300 K without any doping. Furthermore, the introduction of Li^+ doping into 3DPBN further improved H_2 uptake compared to the bare BN nanostructure. This research showcased that 3DPBN overcomes the intrinsic limitations of sorbent materials, achieving a capacity-kinetics-thermodynamics relationship on par with traditional hydrides, while offering superior characteristics [104].

4.2. Power hydrides

Among the known hydrogen storage technologies, hydrogen storage in solid compounds seems to be the most appropriate solution, since it is a safer and more convenient method compared to high-pressure compression and liquefaction technologies. The main solid-state compounds of hydrogen storage technology are metal hydrides, which are represented by simple (binary) metal hydrides, hydrides of intermetallic compounds (alloys) and complex hydrides. Conventional hydrides, exemplified by $LaNi_5H_x$, exhibit low H_2 uptake due to their high density. On the other hand, complex hydrides like $NaAlH_4$ have higher H_2 uptake capabilities, but their slow H_2 release kinetic hinders their practical applications. Chemical hydrides such as $NaBH_4$ have demonstrated impressive performance in terms of both volumetric and gravimetric uptakes. However, their irreversibility poses a significant challenge [105]. Simple metal hydrides, in turn, can be classified according to the type of bond. Non-metal hydrides (Al, Be, Sn, Sb) are covalent. Ionic hydrides include hydrides of alkali and alkaline earth metals (Li, Na, K, Cs, except for Mg). Among binary covalent and ionic hydrides, Al, Be, Na, Li hydrides, which release hydrogen during hydrolysis, are of interest from the point of view of hydrogen storage possibilities. The hydrolysis reaction is irreversible, which is a disadvantage of the method. However, when considering the storage of hydrogen on board a fuel cell vehicle, one should take into account the fact that the exhaust of such a vehicle is water vapor, which can be collected and reused to produce hydrogen on board [106–108].

Metal hydrides include hydrides of transition and rare earth metals (Zn, Ti, Pb, Ni, La, Gd). Hydrides of intermetallic compounds contain atoms of rare earth and transition metals (also Mg, Ca, Al, etc.). Metal hydrides have a high bulk density with respect to hydrogen, but the mass capacity does not exceed 3%. For hydrogen storage, such intermetallic compounds as $LaNi_5$, Ti_2Ni, ZrV_2, TiFe are of interest. Complex hydrides include aluminum hydrides (containing AlH_4), metal borohydrides (containing BH_4), hydrides based on metal amides, and others. They actively interact with water, releasing hydrogen. Aluminum hydrides, borohydrides, hydrides based on amides have both

high bulk and high mass density (for example, 10.6 wt.% for $LiAlH_4$, 18.5 wt.% for $LiBH_4$). The hydrogen uptake and desorption rates for this system are low, so Ti-based catalysts are used. Alanates are actively researched; however, there are still problems of cost and unsafe use of them (these substances are classified as "A" for fire and explosion hazards). In addition, the introduction of borohydrides is hampered by the following disadvantages: thermodynamic stability and the possibility of the formation of toxic volatile borohydrides [101,102].

Magnesium hydride (MgH_2) is a promising material for on-board hydrogen storage due to its high capacity, low cost, and abundant magnesium resources. However, its practical application is limited by poor dehydrogenation ability and cycling stability. This study focuses on investigating influences and mechanisms of thin pristine magnesium oxide (MgO) and transition metal (TM)-dissolved Mg(TM)O layers (TM = Ti, V, Nb, Fe, Co, Ni) on the hydrogen desorption and reversible cycling properties of MgH_2 using first-principles calculations. The results reveal that both thin pristine MgO and Mg(TM)O layers weaken the Mg–H bond strength in MgH_2, leading to decreased structural stability and hydrogen desorption energy. Among the TM-dissolved MgO layers, the Mg(Nb)O layer exhibits the most pronounced destabilization effect on MgH_2. Additionally, the Mg(Nb)O layer demonstrates a long-acting confinement effect on MgH_2 due to stronger interfacial bonding strength between Mg(Nb)O and MgH_2 and the lower brittleness of Mg(Nb)O itself. It provides valuable insights into the design of modified MgH_2 systems for improved hydrogen storage, opening up possibilities for the development of more efficient and stable MgH_2-based hydrogen storage materials [111]. Figure 6a shows promising materials for hydrogen storage. Figures 6b and 6c show pressure-composition isotherms of hydrogen in absorption processes, MgH_2 composite samples at 300 °C at 0.1 bar H_2.

The resulting MgH_2 + 10 wt.% Mn_3O_4/ZrO_2 composite exhibited significant improvements in hydrogen desorption and absorption properties. The composite started releasing hydrogen at a much lower temperature of 219 °C, which was 111 °C lower compared to the as-synthesized MgH_2. At 250 °C, the composite released 6.4 wt.% hydrogen within 10 minutes, while the as-synthesized MgH_2 only released 1.4 wt.% hydrogen even at 335 °C. Furthermore, the dehydrogenated MgH_2 + 10 wt.% Mn_3O_4/ZrO_2 composite demonstrated hydrogen uptake at room temperature, absorbing 6.0 wt.% hydrogen when heated to 250 °C under 3 MPa H_2 pressure and 4.1 wt.% hydrogen within 30 minutes at 100 °C under the same pressure. The MgH_2 + 10 wt.% Mn_3O_4/ZrO_2 composite also exhibited lower activation

energy values for both dehydrogenation and rehydrogenation processes compared to the as-synthesized MgH_2. The activation energy for dehydrogenation was reduced to 64.52 ± 13.14 kJ/mol, while the activation energy for rehydrogenation was decreased to 16.79 ± 4.57 kJ/mol. These lowered activation energy values significantly contributed to the enhanced hydrogen desorption and absorption properties of MgH_2. The incorporation of Mn_3O_4/ZrO_2 nanoparticles into MgH_2 through a simple synthesis method resulted in a composite material with improved hydrogen sorption performance [114].

The addition of graphene oxide-based porous carbon (GC) and titanium chloride ($TiCl_3$) to the MgH_2 system leads to remarkable improvements in dehydrogenation temperature and kinetics. By utilizing a chemical impregnation, hydrogenation, and ball milling process, the MgH_2/GC-$TiCl_3$ composite sample exhibits enhanced hydrogen storage performance. For instance, it can reversibly release approximately 7.6 wt.% of hydrogen at 300 °C within 9 minutes. The average dehydrogenation rate of MgH_2/GC-$TiCl_3$ is significantly faster compared to systems containing only nanoconfined or catalytic MgH_2. The combined analyses of phase, microstructure, and chemical state reveal that GC and $TiCl_3$ play a crucial role in promoting the hydrogen storage properties. GC acts as a foreign scaffold material that tailors the nanophase structure of the MgH_2 composite, while $TiCl_3$ functions as an effective catalyst. This synergistic effect of nanoconfinement and catalysis leads to the improved hydrogen storage performance of the MgH_2/GC-$TiCl_3$ composite [113].

In addition, carbon-supported nanocrystalline TiO_2 (TiO_2@C) has demonstrated excellent catalytic activity in the hydrogen storage reaction of MgH_2. The addition of a small amount of TiO_2@C significantly lowers the dehydrogenation operating temperatures of MgH_2. For example, the MgH_2-10 wt.% TiO_2@C sample begins releasing hydrogen at 205 °C, which is 95 °C lower than the temperature required for pristine MgH_2. At 300 °C, the sample containing 10 wt.% TiO_2@C rapidly releases 6.5 wt.% hydrogen within a short time of 7 minutes. Overall, the addition of TiO_2@C as a catalyst in MgH_2 significantly enhances the hydrogen storage properties of MgH_2. The catalytic effect of TiO_2@C results in reduced dehydrogenation temperatures, rapid hydrogen release, improved hydrogen uptake at room temperature and under pressure, and reduced activation energies for both dehydrogenation and hydrogenation processes [111].

The chemical interaction between magnesium hydride (MgH_2) and the additive titania (TiO_2) and its impact on the dehydrogenation process of MgH_2. Through quantitative X-ray diffraction analysis of ball-milled samples of
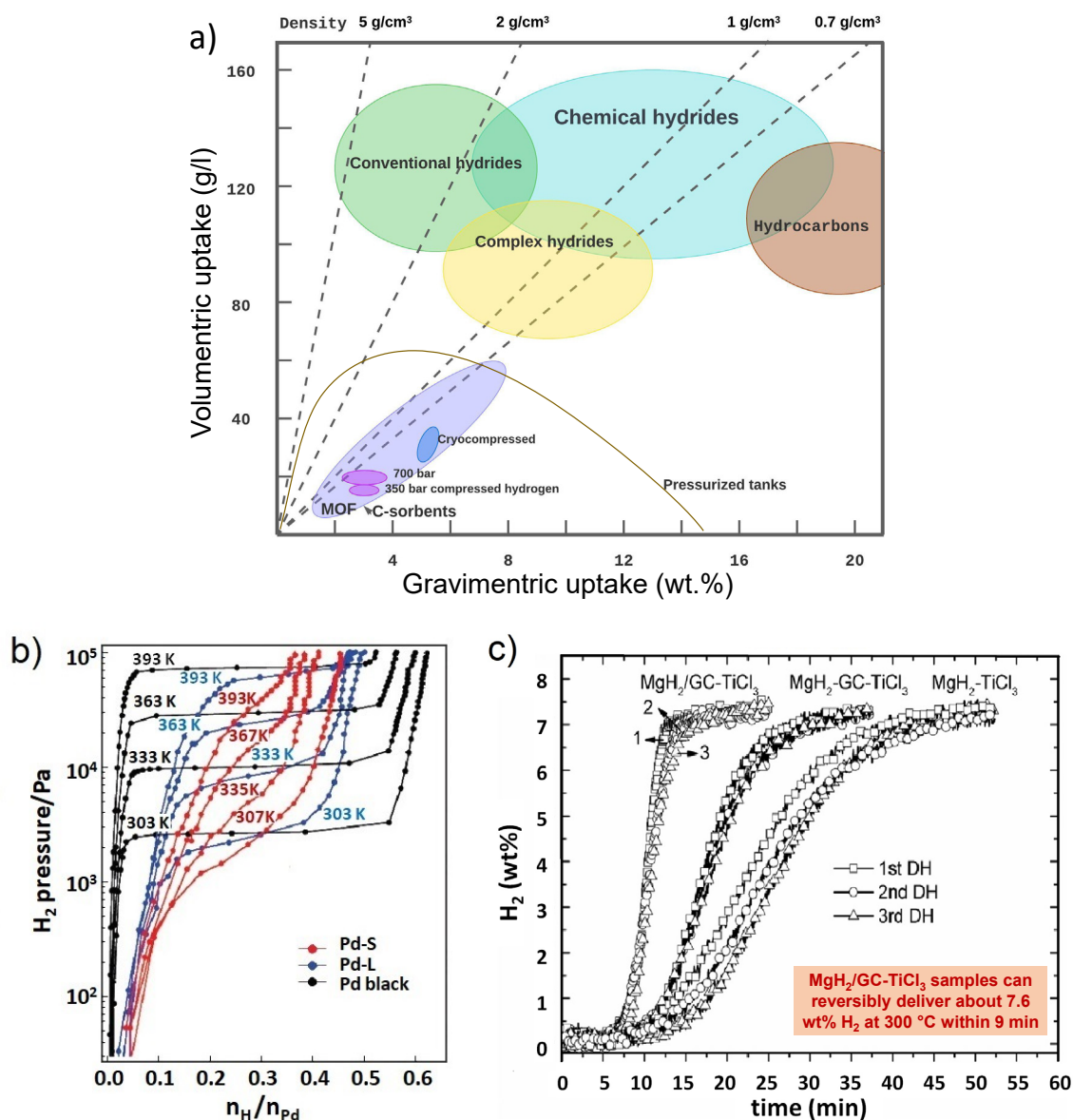
Fig. 6. a) Promising hydrogen storage materials. Adapted from Ref. [103]. b) Hydrogen pressure-composition isotherms in absorption processes (Pd-S – small nanoparticles, Pd-L – large nanoparticles, Pd black – commercial samples). Adapted with permission from Ref. [112], © 2008 American Chemical Society. c) Cyclic dehydriding curves of the MgH_2-$TiCl_3$, MgH_2/GC-$TiCl_3$ and MgH_2-GC-$TiCl_3$ composite samples (GC – graphene oxide-based porous carbon). Adapted from Ref. [113].

$MgH_2 + xTiO_2$ (where $x = 0.25$, 0.33, 0.5, and 1), it is determined that Ti-substituted MgO is the primary reaction product in all the resulting powders. It is found that the effectiveness of Ti-substituted MgO as a catalyst for MgH_2 depends on the concentration of Ti in the rock salt structure of $Mg_xTi_yO_{x+y}$. The findings shed light on the role of TiO_2 in chemically modified MgO and its impact on the dehydrogenation process of MgH_2 [115].

In general, this industry is booming, but so far, no metal hydride has met all the requirements in terms of hydrogen storage capacity, reaction enthalpy and reaction kinetics for efficient hydrogen storage in the required operating temperature ranges [116,117]. In particular, this is due to the fact that during reversible storage of hydrogen in hydrides of

metals and intermetallic compounds, an increase in the pressure of gaseous hydrogen and a decrease in temperature shift the equilibrium towards the formation of a hydride (the reaction proceeds with the release of heat), with a decrease in pressure and an increase in temperature, dissociation occurs (reaction goes with the absorption of heat).

The main methods for eliminating these shortcomings are nanostructuring, adding destabilizing agents, using a catalyst, and doping. The size effect of doping plays a crucial role in the production of catalyzed nanocomposites. Nanoparticles of various metals and their compounds, such as Ni, Zn, Ti, Na, TiF_3, NbF_5, are used as catalysts. Moreover, binary hydride systems such as $LiAlH_4$-MgH_2 and $LiAlH_4$-$LiBH_4$ show improved de/hydrogenation

characteristics compared to their individual hydrides. Strengthening of the hydrogen sorption properties is also associated with the formation of intermediate compounds during dehydrogenation, including Li-Mg, Mg-Al, Al-B and Mg-Al-B alloys, which change the thermodynamics of reactions due to a change in the dehydrogenation path [118,119].

Unfortunately, nanoscale materials are prone to agglomeration and even sintering at elevated temperatures. For some hydrides, the synthesis of nanoparticles is, in principle, very difficult to implement. To overcome these obstacles, a limiting nanoframework is used, formed by microporous activated carbon, graphene, polymer and carbon nanotubes, hollow carbon nanospheres, organometallic frame materials, etc. [94,120–123]. Such compounds are called intercalation. Intercalation of layered materials is a highly efficient method for controlling their reactive, adsorption, catalytic, and other properties.

Intercalation processes are reversible chemical reactions in which "guest" molecules (atoms, ions) are introduced into the matrix of a solid. A characteristic feature of the process of intercalation into layered structures is the introduction of guest molecules into the interlayer space. This leads to the fact that molecules differing in size and geometry can intercalate into the same layered matrix. For example, the relative ease of introducing various ions into the interlayer space of hydrated titanium dioxide is of scientific interest in creating structures with a controlled composition and size of the interlayer space, which are of interest as inorganic sorbents with selective ion-exchange properties [124].

In the field of metal hydrides, M.Y. Song [125] made significant advancements by developing a metal hydride based on magnesium (MgH_2) with unique properties. This MgH_2 material exhibited a high hydrogen storage capacity of more than 110 H_2 g/l and a gravimetric capacity of 7.6 wt.%. Various approaches were explored, including reducing the particle size of MgH_2, alloying magnesium with other transition metals or their oxides, and utilizing catalysts to enhance the hydrogen storage kinetics. M. Vogt and his research group [92] made further progress in this area by developing a power paste formulation using magnesium salt powder/ester. The power paste approach offers a potential alternative for hydrogen storage, providing improved energy density and addressing the challenges associated with traditional storage methods. The reaction of magnesium hydride (MgH_2) with water holds great promise for hydrogen generation in fuel cell applications. MgH_2 is an attractive choice as it is affordable, non-toxic, has a long shelf life, and exhibits an extremely high hydrogen storage capacity of up to 15.3 wt.% in hydrolysis reactions. However, pure MgH_2 reacts very slowly and incompletely with water. Previous attempts to improve the

hydrogen release kinetics and yield often involved the addition of large amounts of Brønsted acids, high-energy ball milling, or expensive noble metal catalysts. This power paste exhibited a higher energy density compared to advanced electrical batteries [126].

4.3. High-entropy alloys

The research on high-entropy alloys (HEAs) for hydrogen storage has shown promising results. In a study by Kao et al. [127], the $FeMnCoTi_xV_yZr_z$ HEA was investigated, where Fe, Mn, Co, Ti, V, and Zr were the constituent elements. The HEA exhibited a single C14 Laves structure, with Zr and Ti occupying the A sites and Fe, Mn, Co, and V located at the B sites. Different variations of the HEA were studied, such as $FeMnCoTi_{0.5–2.5}VZr$, $FeMnCoTiV_{0.4–3.0}Zr$, and $FeMnCoTiVZr_{0.4–3.0}$, all of which showed single C14 Laves phases. By adjusting the proportions of V, Zr, and Ti, the hydrogen absorption and desorption properties of these HEAs were enhanced without altering the original crystal structure. For example, $FeMnCoTi_2VZr$ exhibited a maximum hydrogen storage capacity $(H/M)_{max}$ of 1.8 wt.% at room temperature. The kinetics of hydrogen absorption and the time required to reach 90% of the absorption capacity $(t_{0.9})$ were also investigated. The size of the interstitial sites was found to be a crucial factor in determining the plateau pressure. Introducing Ti or Zr into the alloys enlarged the interstitial sites and led to the expansion of the crystal lattice, resulting in lower compressive atomic stresses. Consequently, the $t_{0.9}$ value and plateau pressure of $FeMnCoTi_xVZr$ and $FeMnCoTiVZr_z$ decreased as the values of x and z increased. Similar studies were conducted on FeMnCrTiVZr HEAs by Chen et al. [128], who found that substituting Cr for Co enhanced the hydrogen absorption properties.

Edalati et al. [129] investigated a C14 Laves structure of FeMnCrNiTiZr, which demonstrated an $(H/M)_{max}$ of 1.7 wt.% with fast kinetics at room temperature without requiring any activation treatment. They highlighted three design criteria for FeMnCrNiTiZr to enable reversible hydrogen storage at room temperature: (i) a total valence-electron concentration (VEC) of 6.4 in HEAs; (ii) selecting the AB_2 system to reduce the hydrogen binding energy by increasing the number of inert elements around the octahedral sites (A and B referring to the elements that react and do not react with hydrogen, respectively); and (iii) achieving single-phase thermodynamic stability. Kunce et al. [130] synthesized a C14 Laves structure-dominated FeCrNiTiVZr using the laser engineered net shaping (LENS) process. The $(H/M)_{max}$ reached 1.81 wt.% after synthesis and 1.56 wt.% after additional heat treatment. Zadorozhnyy et al. [131] produced the same HEA via an
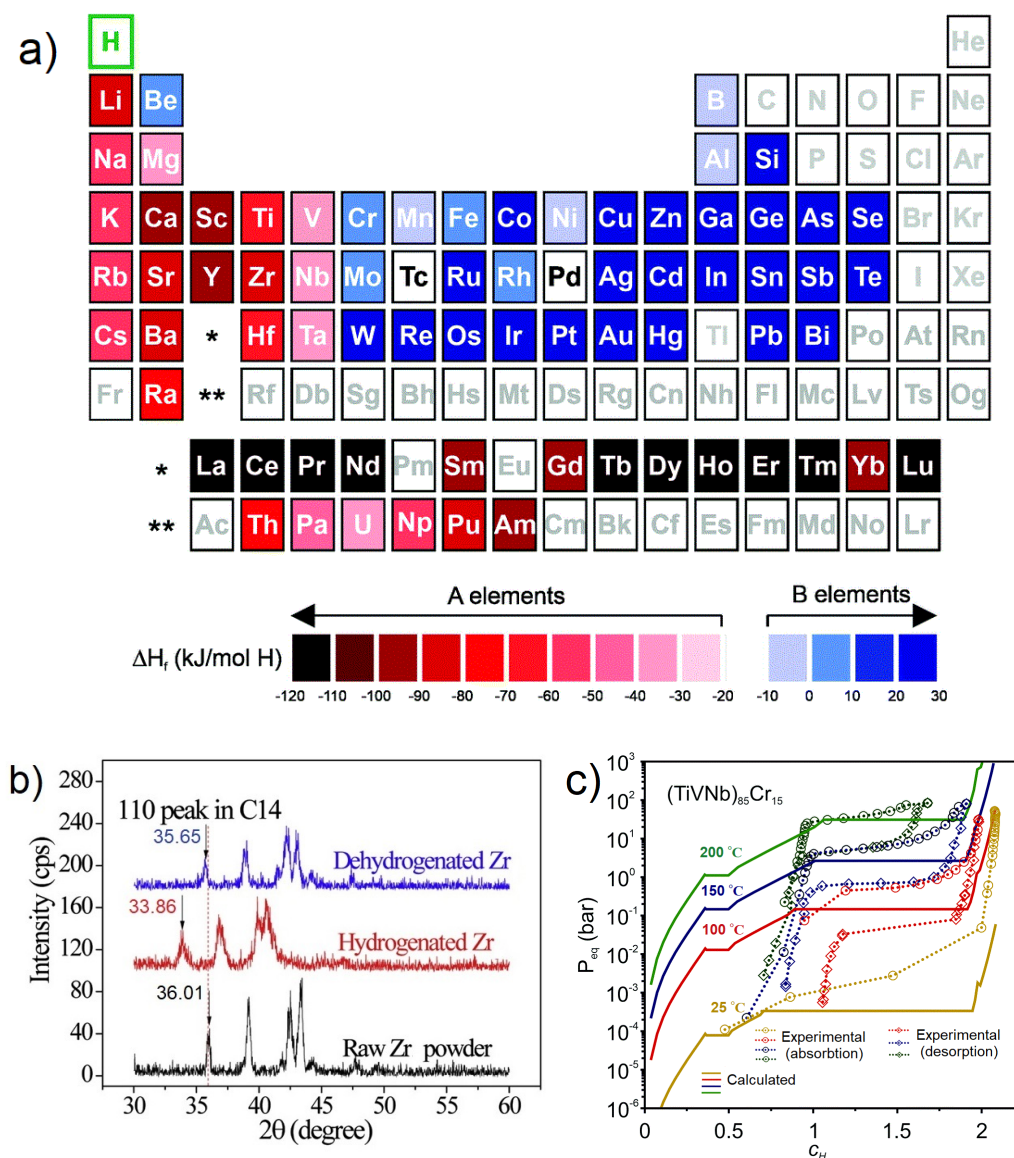
Fig. 7. a) Periodic table with relative subdivision of the A- and B-type elements, taking into account the grouping according to the enthalpies of formation of the binary metal hydrides. Reprinted under Creative Commons Attribution 3.0 Unported License from Ref. [132], © 2021 The Royal Society of Chemistry; b) XRD patterns for hydrogenated, dehydrogenated, and as-cast (raw) powder Zr. Adapted from Ref. [127]; c) Experimental PCTs of the $(TiVNb)_{85}Cr_{15}$ alloy measured at 25 °C (298 K) (only absorption), 100 °C (373 K) (H$_2$ a/d), 150 °C (423 K) and 200 °C (473 K) compared with the calculated PCT using the thermodynamic model. Adapted from Ref. [133].

arc melting-based rapid solidification process. The highest hydrogen storage capacity achieved was 1.6 wt.% during the first hydrogenation, followed by a reduction to 1.3–1.4 wt.% in subsequent cycles at ambient temperature. Figure 7a shows a periodic table with a relative subdivision of A- and B-type elements, taking into account the grouping according to the enthalpies of formation of binary metal hydrides. X-ray diffraction patterns of hydrogenated, dehydrogenated, and raw Zr powder are shown in Figure 7b. The experimental pressure-composition-temperature (PCT) diagram of the $(TiVNb)_{85}Cr_{15}$ alloy compared to the calculated PCT using the thermodynamic model is shown in Figure 7c.

BCC high-entropy alloys (HEAs) have been extensively investigated as hydrogen storage materials, particularly those composed of refractory elements. These alloys have shown the ability to absorb significant amounts of hydrogen, forming hydride phases with a maximum hydrogen-to-metal (H/M) ratio of 2. Sahlberg et al. [133] reported on a bcc-type TiNbVZrHf HEA that could be hydrogenated to an H/M ratio of 2.5 in a body-centered tetragonal (BCT) structure. The high hydrogen storage capacity observed in this HEA was attributed to the lattice distortion in the alloy. Karlsson et al. [134] also studied the same composition

HEA and observed a phase transition from BCC to BCT structure, again achieving a maximum H/M ratio of 2.5. In a recent study by Nygard et al. [135], a series of quaternary and quinary refractory TiNbV-based alloys were investigated, including TiNbVX (X = Zr, Cr, Hf, Mo, Ta), TiNbVZrHf, TiNbVCrMo, and TiNbVCrTa. The study highlighted the importance of valence electron concentration (VEC) in destabilizing hydrides. The volume expansion of each metal atom in the alloy hydrides was found to increase linearly with the VEC of the alloy. Additionally, the onset temperature for hydrogen desorption exhibited a linear decrease with VEC. Other BCC HEAs, such as FeCoNiMgTiZr, FeMnNiCrAlW, and TiZrHfScMo, have also been investigated as hydrogen storage materials. In addition to the BCC and C14 Laves structures, HEAs with mixed phases have been reported as well. Multiphase alloys, such as $(FeV)_{60}(CoTiCr)_{40-x}Zr_x$ ($0 \leq x \leq 2$), have shown the ability to quickly absorb hydrogen without requiring an activation process, even at room temperature [132,136]. The HEAs have demonstrated their utility in various applications, including catalysis and energy storage. Notable HEAs, such as TiVZrNbHf, TiZrHfMoNb, TiZrNbFeNi, HfNbTiVZr, and TiZrNbTa, have been synthesized and shown appreciable capacity for hydrogen storage [132,136]. In a study by Bondesgaard et al. [137], a solvothermal method was developed as a simple and general production method for metal nanoalloys with different combinations and compositions. This method was found to produce phase-pure high-entropy nanoalloys, such as $Pt_{0.33}Pd_{0.33}Rh_{0.33}$, $Pt_{0.33}Rh_{0.33}Ru_{0.33}$, $Pt_{0.25}Pd_{0.25}Rh_{0.25}Ru_{0.25}$, and $Pt_{0.20}Pd_{0.20}Ir_{0.20}Rh_{0.20}Ru_{0.20}$, covering the entire composition range. This wet-chemical synthesis approach, combined with the selection of appropriate metal precursors and solvents, allows for the tuning of nanoalloy properties for hydrogen storage applications [137]. A recent patent [138] has discussed new high-entropy alloys (HEAs) capable of absorbing and desorbing dihydrogen under ambient temperature and pressure conditions, with a large number of charging and discharging cycles. This development has brought significant progress to the field, as previous reports struggled to demonstrate efficient hydrogen absorption and desorption under ambient conditions.

Titanium and its compounds, including oxides, are actively used in hydrogen storage devices. For example, hydrogen sorbents are being developed, consisting of nanostructures (fullerenes) with Ti atoms on the surface, to which hydrogen easily attaches. In the technology of solid-state storage of hydrogen based on hydride pastes, nanostructured titanium dioxide is proposed to be used as a catalyst for hydrogen absorption and desorption reactions. Titanium is found quite often in the composition of intermetallic compounds, demonstrating good capacitive characteristics and resistance to cyclic loads (charge/discharge).

5. CONCLUSION

Despite the fact that the presented technologies have been intensively developed for a long time in the direction of hydrogen production and storage, they still do not find widespread use in the energy sector and are at different stages of implementation in the industrial sector. This is due to a number of problems, both economic and technological. Science-intensive technologies for the production and storage of hydrogen are still quite expensive for their widespread use. Currently, only technologies for producing brown and gray hydrogen (methane reforming and coal gasification) are used in the energy sector, and technologies for producing turquoise and blue hydrogen (methane pyrolysis and technology with a process that uses carbon capture) are also gradually gaining momentum.

High-performance hydrogen carriers related to green energy are well positioned to enter the market in place of fossil analogues. Photoelectrochemical water splitting is very attractive for producing green hydrogen. However, this method is still under development, as the efficiency of water splitting is limited by complex solid-liquid interface reactions, including slow gas desorption and significant recombination of photogenerated charges. Research work in the field of increasing the efficiency of the photoelectrochemical process is aimed at modifying the surfaces of electrodes, including the modification of the surface of cocatalysts for the reaction of hydrogen evolution; surface passivation and application of a protective layer for the water reduction reaction; as well as the selection of the composition of the electrolyte.

High-entropy alloys (HEAs) and power paste materials, such as magnesium hydrides, have emerged as promising candidates for hydrogen storage. These materials can form hydrides with hydrogen-to-metal ratios of up to 2.5 and exhibit exceptional hydrogen storage capabilities. HEAs consist of at least five principal elements with varying atomic percentages, forming single-phase solid solutions with different crystal structures. The unique composition and crystal structures of HEAs contribute to their remarkable hydrogen storage properties. Solid-state hydrogen storage offers advantages like reduced transportation risks and the ability to store hydrogen in residential settings. This alternative approach is gaining traction in the hydrogen transportation sector, addressing challenges associated with high-compressed hydrogen tanks in smaller vehicles. Portable hydrogen generators based on power paste or HEAs provide a more compact and efficient solution for hydrogen storage and transportation, making hydrogen fuel more accessible for various applications, including small vehicles. These advancements hold the potential to accelerate the adoption of hydrogen

as a practical and sustainable energy source. The development of solid-state hydrogen storage materials, including HEAs, power paste materials, and additive-modified hydrides, shows promise in improving the efficiency, safety, and practicality of hydrogen storage.

Titanium dioxide has favorable corrosion resistance, high mechanical strength and excellent biocompatibility. To date, extensive research has been carried out to fabricate reliable and controllable TiO_2 nanostructures using various nanoengineering strategies. For example, nanoengineering of the Ti surface can thicken the TiO_2 layer and provide ordering of various titanium dioxide nanostructures, such as nanotubes and nanopores. Due to favorable characteristics, ordered TiO_2 nanostructures are widely studied in the field of catalysis and energetics.

ACKNOWLEDGEMENTS

REFERENCES

[1] S. van Renssen, *The hydrogen solution?*, Nat. Clim. Chang., 2020, vol. 10, no. 9, pp. 799–801.

[2] P.J. Megia, A.J. Vizcaino, J.A. Calles, A. Carrero, *Hydrogen Production Technologies: From Fossil Fuels toward Renewable Sources. A Mini Review*, Energy Fuels, 2021, vol. 35, no. 20, pp. 16403–16415.

[3] J.O. Abe, A.P.I. Popoola, E. Ajenifuja, O.M. Popoola, *Hydrogen energy, economy and storage: Review and recommendation*, Int. J. Hydrog. Energy, 2019, vol. 44, no. 29, pp. 15072–15086.

[4] T.E. Lipman, *Hydrogen Production Science and Technology*, in: *Fuel Cells and Hydrogen Production. Encyclopedia of Sustainability Science and Technology Series*, ed. by T. Lipman. A. Weber, Springer, New York, 2019, pp. 783–798.

[5] A.M. Abdalla, S. Hossain, O.B. Nisfindy, A.T. Azad, M. Dawood, A.K. Azad, *Hydrogen production, storage, transportation and key challenges with applications: A review*, Energy Convers. Manag., 2018, vol. 165, pp. 602–627.

[6] L. Barelli, G. Bidini, F. Gallorini, S. Servili, *Hydrogen production through sorption-enhanced steam methane reforming and membrane technology: A review*, Energy, 2008, vol. 33, no. 4, pp. 554–570.

[7] A. Borgschulte, *The hydrogen grand challenge*, Front. Energy Res., 2016, vol. 4, art. no. 11.

[8] M. Kaur, K. Pal, *Review on hydrogen storage materials and methods from an electrochemical viewpoint*, J. Energy Storage, 2019, vol. 23, pp. 234–249.

[9] M. Mohan, V.K. Sharma, E.A. Kumar, V. Gayathri, *Hydrogen storage in carbon materials—A review*, Energy Storage, 2019, vol. 1, no. 2, art. no. e35.

[10] A. Eftekhari, B. Fang, *Electrochemical hydrogen storage: Opportunities for fuel storage, batteries, fuel cells, and supercapacitors*, Int. J. Hydrog. Energy, 2017, vol. 42, no. 40, pp. 25143–25165.

[11] H.L. Yip, A. Srna, A.C.Y. Yuen, S. Kook, R.A. Taylor, G.H. Yeoh, P.R. Medwell, Q.N. Chan, *A review of hydrogen direct injection for internal combustion engines: Towards carbon-free combustion*, Appl. Sci., 2019, vol. 9, no. 22, art. no. 4822.

[12] M. Handwerker, J. Wellnitz, H. Marzbani, *Comparison of Hydrogen Powertrains with the Battery Powered Electric Vehicle and Investigation of Small-Scale Local Hydrogen Production Using Renewable Energy*, Hydrogen, vol. 2, no. 1, pp. 76–100.

[13] Y. Wang, Y. He, Q. Lai, M. Fan, *Review of the progress in preparing nano TiO2: an important environmental engineering material*, J. Environ. Sci., 2014, vol. 26, no. 11, pp. 2139–2177.

[14] J. Geng, D. Yang, J. Zhu, D. Chen, Z. Jiang, *Nitrogen-doped TiO2 nanotubes with enhanced photocatalytic activity synthesized by a facile wet chemistry method*, Mater. Res. Bull., 2009, vol. 44, no. 1, pp. 146–150.

[15] L.C. Jiang, W.D. Zhang, *Electrodeposition of TiO2 nanoparticles on multiwalled carbon nanotube arrays for hydrogen peroxide sensing*, Electroanalysis, 2009, vol. 21, no. 8, pp. 988–993.

[16] L. González-Reyes, I. Hernández-Pérez, L. Díaz-Barriga Arceo, H. Dorantes-Rosales, E. Arce-Estrada, R. Suárez-Parra, J.J. Cruz-Rivera, *Temperature effects during Ostwald ripening on structural and bandgap properties of TiO2 nanoparticles prepared by sonochemical synthesis*, Mater. Sci. Eng. B, 2010, vol. 175, no. 1, pp. 9–13.

[17] E. Podlesnov, M.G. Nigamatdianov, M.V Dorogov, *Review of Materials for Electrodes and Electrolytes of Lithium Batteries*, Rev. Adv. Mater. Technol., 2022, vol. 4, no. 4, pp. 39–61.

[18] E. Podlesnov, M.G. Nigamatdianov, A.O. Safronova, M.V. Dorogov, *Lithium Polymer Battery with PVDF-based Electrolyte Doped with Copper Oxide Nanoparticles: Manufacturing Technology and Properties*, Rev. Adv. Mater. Technol., 2021, vol. 3, no. 3, pp. 27–31.

[19] P.S. Basavarajappa, S.B. Patil, N. Ganganagappa, K.R. Reddy, A.V. Raghu, C.V. Reddy, *Recent progress in metal-doped TiO2, non-metal doped/codoped TiO2 and TiO2 nanostructured hybrids for enhanced photocatalysis*, Int. J. Hydrog. Energy, 2020, vol. 45, no. 13, pp. 7764–7778.

[20] S. Chang, C. Hou, P. Lo, C. Chang, *Preparation of phosphated Zr-doped TiO2 exhibiting high photocatalytic activity through calcination of ligand-capped nanocrystals*, Appl. Catal. B, 2009, vol. 90, no. 1–2, pp. 233–241.

[21] W. Zhao, S. Liu, S. Zhang, R. Wang, K. Wang, *Preparation and visible-light photocatalytic activity of N-doped TiO2 by plasma-assisted sol-gel method*, Catal. Today, 2019, vol. 337, pp. 37–43.

[22] F.K.M. Alosfur, M.H.H. Jumali, S. Radiman, N.J. Ridha, M.A. Yarmo, A.A. Umar, *Modified microwave method for the synthesis of visible light-responsive TiO2/MWCNTs nanocatalysts*, Nanoscale Res. Lett., 2013, vol. 8, no. 1, art. no. 346.

[23] Y.C. Chang, C.J. Zeng, C.Y. Chen, C.Y. Tsay, G.J. Lee, J.J. Wu, *NiS/Pt loaded on electrospun TiO2 nanofiber with enhanced visible-light-driven photocatalytic hydrogen production*, Mater. Res. Bull., 2023, vol. 157, art. no. 112041.

[24] N. Bayal, P. Jeevanandam, *Synthesis of TiO2-MgO mixed metal oxide nanoparticles via a sol-gel method*

and studies on their optical properties, Ceram. Int., 2014, vol. 40, no. 10, pp. 15463–15477.

[25] L.M. Dorogin, M.V. Dorogov, S. Vlassov, A.A. Vikarchuk, A.E. Romanov, *Whisker Growth and Cavity Formation at the Microscale*, Rev. Adv. Mater. Technol., 2020, vol. 2, no. 1, pp. 1–31.

[26] S. Xu, X. Sun, Y. Gao, M. Yue, Q. Yue, B. Gao, *Solvent effects on microstructures and properties of three-dimensional hierarchical TiO2 microsphere structures synthesized via solvothermal approach*, J. Solid State Chem., 2017, vol. 253, pp. 167–175.

[27] M. Dorogov, A. Kalmykov, L. Sorokin, A. Kozlov, A. Myasoedov, D. Kirilenko, N. Chirkunova, A. Priezzheva, A. Romanov, E.C. Aifantis, *CuO nanowhiskers: preparation, structure features, properties, and applications*, Mater. Sci. Technol., 2018, vol. 34, no. 17, pp. 2126–2135.

[28] X. Chen, S.S. Mao, *Titanium dioxide nanomaterials: Synthesis, properties, modifications and applications*, Chem. Rev., 2007, vol. 107, no. 7, pp. 2891–2959.

[29] V. Kumaravel, S. Mathew, J. Bartlett, S.C. Pillai, *Photocatalytic hydrogen production using metal doped TiO2: A review of recent advances*, Appl. Catal. B, 2019, vol. 244, pp. 1021–1064.

[30] G. Dai, J. Yu, G. Liu, *Synthesis and enhanced visible-light photoelectrocatalytic activity of p-n junction BiOI/TiO2 nanotube arrays*, J. Phys. Chem. C, 2011, vol. 115, no. 15, pp. 7339–7346.

[31] M.R. Hoffmann, S.T. Martin, W. Choi, D.W. Bahnemann, *Environmental Applications of Semiconductor Photocatalysis*, Chem. Rev., 1995, vol. 95, no. 1, pp. 69–96.

[32] I. Gurrappa, L. Binder, *Electrodeposition of nanostructured coatings and their characterization - A review*, Sci. Technol. Adv. Mater., 2008, vol. 9, no. 4, art. no. 043001.

[33] Y. Jiao, C. Peng, F. Guo, Z. Bao, J. Yang, L. Schmidt-Mende, R. Dunbar, Y. Qin, Z. Deng, *Facile synthesis and photocatalysis of size-distributed TiO2 hollow spheres consisting of {116} plane-oriented nanocrystallites*, J. Phys. Chem. C, 2011, vol. 115, no. 14, pp. 6405–6409.

[34] Q.E. Zhao, W. Wen, Y. Xia, J.M. Wu, *Photocatalytic activity of TiO2 nanorods, nanowires and nanoflowers filled with TiO2 nanoparticles*, Thin Solid Films, 2018, vol. 648, pp. 103–107.

[35] H. Zhang, J.F. Banfield, *Structural Characteristics and Mechanical and Thermodynamic Properties of Nanocrystalline TiO2*, Chem. Rev., 2014, vol. 114, no. 19, pp. 9613–9644.

[36] J.-G. Li, T. Ishigaki, X. Sun, *Anatase, Brookite, and Rutile Nanocrystals via Redox Reactions under Mild Hydrothermal Conditions: Phase-Selective Synthesis and Physicochemical Properties*, J. Phys. Chem. C, 2007, vol. 111, no. 13, pp. 4969–4976.

[37] D. R. Eddy, M.D. Permana, L.K. Sakti, G.A.N. Sheha, Solihudin, S. Hidayat, T. Takei, N. Kumada, I. Rahayu, *Heterophase Polymorph of TiO2 (Anatase, Rutile, Brookite, TiO2 (B)) for Efficient Photocatalyst: Fabrication and Activity*, Nanomater., 2023, vol. 13, no. 4, art. no. 704.

[38] T.A. Kandiel, A. Feldhoff, L. Robben, R. Dillert, D.W. Bahnemann, *Tailored Titanium Dioxide Nanomaterials: Anatase Nanoparticles and Brookite Nanorods as Highly Active Photocatalysts*, Chem. Mater., 2010, vol. 22, no. 6, pp. 2050–2060.

[39] R. Buonsanti, V. Grillo, E. Carlino, C. Giannini, T. Kipp, R. Cingolani, P.D. Cozzoli, *Nonhydrolytic Synthesis of High-Quality Anisotropically Shaped Brookite TiO2 Nanocrystals*, J. Am. Chem. Soc., 2008, vol. 130, no. 33, pp. 11223–11233.

[40] S.M. Gupta, M. Tripathi, *A review of TiO2 nanoparticles*, Chinese Sci. Bull., 2011, vol. 56, no. 16, pp. 1639–1657.

[41] H.G. Yang, G. Liu, S.Z. Qiao, C.H. Sun, Y.G. Jin, S.C. Smith, J. Zou, H.M. Cheng, G.Q. Lu, *Solvothermal synthesis and photoreactivity of anatase TiO2 nanosheets with dominant {001} facets*, J. Am. Chem. Soc., 2009, vol. 131, no. 11, pp. 4078–4083.

[42] D. Li, H. Haneda, S. Hishita, N. Ohashi, *Visible-Light-Driven N−F−Codoped TiO2 Photocatalysts. 1. Synthesis by Spray Pyrolysis and Surface Characterization*, Chem. Mater., 2005, vol. 17, no. 10, pp. 2588–2595.

[43] S.S. Mali, C.A. Betty, P.N. Bhosale, R.S. Devan, Y.-R. Ma, S.S. Kolekara, P.S. Patil, *Hydrothermal synthesis of rutile TiO2 nanoflowers using Brønsted Acidic Ionic Liquid [BAIL]: Synthesis, characterization and growth mechanism*, CrystEngComm, 2012, vol. 14, no. 6, pp. 1920–1924.

[44] J. Wang, Z. Lin, *Freestanding TiO2 Nanotube Arrays with Ultrahigh Aspect Ratio via Electrochemical Anodization*, Chem. Mater., 2008, vol. 20, no. 4, pp. 1257–1261.

[45] C.U. Bhadra, D. Jonas Davidson, D. Henry Raja, *Fabrication of titanium oxide nanotubes by varying the anodization time*, Mater. Today Proc., 2020, vol. 33, pp. 2711–2715.

[46] A.J. Terezo, E.C. Pereira, *Preparation and characterization of Ti/RuO2-Nb2O5 electrodes obtained by polymeric precursor method*, Electrochim. Acta, 1999, vol. 44, no. 25, pp. 4507–4513.

[47] T. Guo, S. Ivanovski, K. Gulati, *Tuning electrolyte aging in titanium anodization to fabricate nano-engineered implants*, Surf. Coatings Technol., 2022, vol. 447, art. no. 128819.

[48] K. Byrappa, M. Yoshimura, *Handbook of hydrothermal technology : a technology for crystal growth and materials processing.* Noyes Publications, New Jersey, 2001.

[49] B. Gomathi Thanga Keerthana, T. Solaiyammal, S. Muniyappan, P. Murugakoothan, *Hydrothermal synthesis and characterization of TiO2 nanostructures prepared using different solvents*, Mater. Lett., 2018, vol. 220, pp. 20–23.

[50] H.A. Khizir, T.A.H. Abbas, *Hydrothermal synthesis of TiO2 nanorods as sensing membrane for extended-gate field-effect transistor (EGFET) pH sensing applications*, Sens. Actuator A Phys., 2022, vol. 333, art. no. 113231.

[51] Z. Jiang, F. Yang, N. Luo, B.T.T. Chu, D. Sun, H. Shi, T. Xiao, P.P. Edwards, *Solvothermal synthesis of N-doped TiO2 nanotubes for visible-light-responsive photocatalysis*, Chem. Commun., 2008, no. 47, pp. 6372–6374.

[52] L. Andronic, D. Andrasi, A. Enesca, M. Visa, A. Duta, *The influence of titanium dioxide phase composition on dyes photocatalysis*, J. Sol-Gel Sci. Technol., 2011, vol. 58, no. 1, pp. 201–208.

[53] C.P. Lin, H. Chen, A. Nakaruk, P. Koshy, C.C. Sorrell, *Effect of annealing temperature on the photocatalytic activity of TiO2 thin films*, Energy Procedia, 2013, vol. 34, pp. 627–636.

[54] L.T. Jule, K. Ramaswamy, B. Bekele, A. Saka, N. Nagaprasad, *Experimental investigation on the impacts of*

annealing temperatures on titanium dioxide nanoparticles structure, size and optical properties synthesized through sol-gel methods*, Mater. Today Proc., 2021, vol. 45, pp. 5752–5758.

[55] N. Venkatachalam, M. Palanichamy, V. Murugesan, *Sol–gel preparation and characterization of nanosize TiO₂: Its photocatalytic performance*, Mater. Chem. Phys., 2007, vol. 104, no. 2–3, pp. 454–459.

[56] Y. Bessekhouad, D. Robert, J.V. Weber, *Synthesis of photocatalytic TiO₂ nanoparticles: Optimization of the preparation conditions*, J. Photochem. Photobiol. A Chem., 2003, vol. 157, no. 1, pp. 47–53.

[57] B. Li, X. Wang, M. Yan, L. Li, *Preparation and characterization of nano-TiO₂ powder*, Mater. Chem. Phys., 2003, vol. 78, no. 1, pp. 184–188.

[58] A. Wong, W.A. Daoud, H. Liang, Y.S. Szeto, *The effect of aging and precursor concentration on room-temperature synthesis of nanocrystalline anatase TiO₂*, Mater. Lett., 2014, vol. 117, pp. 82–85.

[59] N.V. Chirkunova, M.M. Skryabina, M.V. Dorogov, *Sol-Gel Prepared TiO₂ Photocatalyst*, Rev. Adv. Mater. Technol., 2020, vol. 2, no. 3, pp. 44–50.

[60] M. Kang, S.Y. Lee, C.H. Chung, S.M. Cho, G.Y. Han, B.W. Kim, K.J. Yoon, *Characterization of a TiO₂ photocatalyst synthesized by the solvothermal method and its catalytic performance for CHCl₃ decomposition*, J. Photochem. Photobiol. A, 2001, vol. 144, no. 2–3, pp. 185–191.

[61] C.C. Chung, T.W. Chung, T.C.K. Yang, *Rapid synthesis of titania nanowires by microwave-assisted hydrothermal treatments*, Ind. Eng. Chem. Res., 2008, vol. 47, no. 7, pp. 2301–2307.

[62] R. Skiba, *Competency Standards for Emerging Hydrogen Related Activities*, Open J. Saf. Sci. Technol., 2020, vol. 10, no. 2, pp. 42–52.

[63] V. Kumar, D. Gupta, N. Kumar, *Hydrogen use in internal combustion engine: a review*, Int. J. Adv. Cult. Technol., 2015, vol. 3, no. 2, pp. 87–99.

[64] *The Future of Hydrogen – Analysis – IEA*, URL: https://www.iea.org/reports/the-future-of-hydrogen (accessed 08.06.2023).

[65] M. Hermesmann, T.E. Müller, *Green, Turquoise, Blue, or Grey? Environmentally friendly Hydrogen Production in Transforming Energy Systems*, Prog. Energy Combust. Sci., 2022, vol. 90, art. no. 100996.

[66] H.F. Abbas, W.M.A. Wan Daud, *Hydrogen production by methane decomposition: A review*, Int. J. Hydrog. Energy, 2010, vol. 35, no. 3, pp. 1160–1190.

[67] G.A. Naikoo, F. Arshad, I.U. Hassan, M.A. Tabook, M.Z. Pedram, M. Mustaqeem, H. Tabassum, W. Ahmed, M. Rezakazemi, *Thermocatalytic Hydrogen Production Through Decomposition of Methane-A Review*, Front. Chem., 2021, vol. 9, art. no. 736801.

[68] S. Shiva Kumar, V. Himabindu, *Hydrogen production by PEM water electrolysis – A review*, Mater. Sci. Energy Technol., 2019, vol. 2, no. 3, pp. 442–454.

[69] F.M. Sapountzi, J.M. Gracia, C.J. Weststrate, H.O.A. Fredriksson, J.W. Niemantsverdriet, *Electrocatalysts for the generation of hydrogen, oxygen and synthesis gas*, Prog. Energy Combust. Sci., 2017, vol. 58, pp. 1–35.

[70] C.Y. Wong, W.Y. Wong, K.S. Loh, W.R. Wan Daud, K.L. Lim, M. Khalid, R. Walvekar, *Development of Poly(Vinyl Alcohol)-Based Polymers as Proton Exchange Membranes and Challenges in Fuel Cell Application: A Review*, Polym. Rev., 2020, vol. 60, no. 1, pp. 171–202.

[71] C. Wu, Y. Wu, J. Luo, T. Xu, Y. Fu, *Anion exchange hybrid membranes from PVA and multi-alkoxy silicon copolymer tailored for diffusion dialysis process*, J. Memb. Sci., 2010, vol. 356, no. 1–2, pp. 96–104.

[72] Y. Wu, C. Wu, Y. Li, T. Xu, Y. Fu, *PVA–silica anion-exchange hybrid membranes prepared through a copolymer crosslinking agent*, J. Memb. Sci., 2010, vol. 350, no. 1–2, pp. 322–332.

[73] M. F. Ali, H.S. Cho, C.I. Bernäcker, J. Albers, C. Young-Woo, M.J. Kim, J.H. Lee, C. Lee, S. Lee, W.C. Cho, *A study on the effect of TiO₂ nanoparticle size on the performance of composite separators in alkaline water electrolysis*, J. Memb. Sci., 2023, vol. 678, art. no. 121671.

[74] J.T. Mefford, X. Rong, A.M. Abakumov, W.G. Hardin, S. Dai, A.M. Kolpak, K.P. Johnston, K.J. Stevenson, *Water electrolysis on La₁₋ₓSrₓCoO₃₋δ perovskite electrocatalysts*, Nat. Commun., 2016, vol. 7, art. no. 11053.

[75] P. Mazúr, J. Polonský, M. Paidar, K. Bouzek, *Non-conductive TiO₂ as the anode catalyst support for PEM water electrolysis*, Int. J. Hydrog. Energy, 2012, vol. 37, no. 17, pp. 12081–12088.

[76] J. Han, H. Choi, G. Lee, Y. Tak, J. Yoon, *Electrochemical activity of a blue anatase TiO₂ nanotube array for the oxygen evolution reaction in alkaline water electrolysis*, J. Electrochem. Sci. Technol., 2016, vol. 7, no. 1, pp. 76–81.

[77] R. Li, B. Hu, T. Yu, Z. Shao, Y. Wang, S. Song, *New TiO₂-Based Oxide for Catalyzing Alkaline Hydrogen Evolution Reaction with Noble Metal-Like Performance*, Small Methods, 2021, vol. 5, no. 6, art. no. 2100246.

[78] A. Fujishima, K. Honda, *Electrochemical Photolysis of Water at a Semiconductor Electrode*, Nature, 1972, vol. 238, no. 5358, pp. 37–38.

[79] K. Maeda, *Photocatalytic water splitting using semiconductor particles: History and recent developments*, J. Photochem. Photobiol. C, 2011, vol. 12, no. 4, pp. 237–268.

[80] B. Oral, E. Can, R. Yildirim, *Analysis of photoelectrochemical water splitting using machine learning*, Int. J. Hydrog. Energy, 2022, vol. 47, no. 45, pp. 19633–19654.

[81] Y. Liu, X. Zhang, R. Liu, R. Yang, C. Liu, Q. Cai, *Fabrication and photocatalytic activity of high-efficiency visible-light-responsive photocatalyst ZnTe/TiO₂ nanotube arrays*, J. Solid State Chem., 2011, vol. 184, no. 3, pp. 684–689.

[82] D. Eder, M. Motta, A.H. Windle, *Iron-doped Pt-TiO₂ nanotubes for photo-catalytic water splitting*, Nanotechnol., 2009, vol. 20, no. 5, art. no. 055602.

[83] C. Li, J. Yuan, B. Han, L. Jiang, W. Shangguan, *TiO₂ nanotubes incorporated with CdS for photocatalytic hydrogen production from splitting water under visible light irradiation*, Int. J. Hydrog. Energy, 2010, vol. 35, no. 13, pp. 7073–7079.

[84] X. Chen, L. Liu, P.Y. Yu, S.S. Mao, *Increasing solar absorption for photocatalysis with black hydrogenated titanium dioxide nanocrystals*, Science, 2011, vol. 331, no. 6018, pp. 746–750.

[85] R. Hahn, F. Schmidt-Stein, J. Salonen, S. Thiemann, Y.Y. Song, J. Kunze, V.P. Lehto, P. Schmuki, *Semimetallic TiO₂ nanotubes*, Angew. Chem. Int. Ed., 2009, vol. 48, no. 39, pp. 7236–7239.

[86] S. Masudy-Panah, Y.J.K. Eugene, N.D. Khiavi, R. Katal, X. Gong, *Aluminum-incorporated p-CuO/n-ZnO photo-cathode coated with nanocrystal-engineered TiO2 protective layer for photoelectrochemical water splitting and hydrogen generation*, J. Mater. Chem. A, 2018, vol. 6, no. 25, pp. 11951–11965.

[87] B. Liu, S. Feng, L. Yang, C. Li, Z. Luo, T. Wang, J. Gong, *Bifacial passivation of n-silicon metal–insulator–semiconductor photoelectrodes for efficient oxygen and hydrogen evolution reactions*, Energy Environ. Sci., 2020, vol. 13, no. 1, pp. 221–228.

[88] X. Hou, L. Fan, Y. Zhao, P.D. Lund, Y. Li, *Highly active titanium oxide photocathode for photoelectrochemical water reduction in alkaline solution*, J. Power Sources, 2022, vol. 524, art. no. 231095.

[89] C.J. Webb, *A review of catalyst-enhanced magnesium hydride as a hydrogen storage material*, J. Phys. Chem. Solids, 2015, vol. 84, no. 1, pp. 96–106.

[90] R. Prabhukhot Prachi, M. Wagh Mahesh, C. Gangal Aneesh, *A Review on Solid State Hydrogen Storage Material*, Adv. Energy Power, 2016, vol. 4, no. 2, pp. 11–22.

[91] R. Chamoun, U.B. Demirci, P. Miele, *Cyclic dehydrogenation-(Re)hydrogenation with hydrogen-storage materials: An overview*, Energy Technol., 2015, vol. 3, no. 2, pp. 100–117.

[92] M. Vogt, F. Heubner, *PowerPaste for off-grid power supply*, Fraunhofer Inst. Manuf. Technol. Adv. Mater., Branch Lab Dresden, 2022.

[93] J. Wang, J. Zhang, Y. Hu, H. Jiang, C. Li, *Activating multisite high-entropy alloy nanocrystals via enriching M–pyridinic N–C bonds for superior electrocatalytic hydrogen evolution*, Sci. Bull., 2022, vol. 67, no. 18, pp. 1890–1897.

[94] F. Li, X. Jiang, J. Zhao, S. Zhang, *Graphene oxide: A promising nanomaterial for energy and environmental applications*, Nano Energy, 2015, vol. 16, pp. 488–515.

[95] X. Zhang, R.B. Lin, J. Wang, B. Wang, B. Liang, T. Yildirim, J. Zhang, W. Zhou, B. Chen, *Optimization of the Pore Structures of MOFs for Record High Hydrogen Volumetric Working Capacity*, Adv. Mater., 2020, vol. 32, no. 17, art. no. 1907995.

[96] A. Züttel, *Materials for Hydrogen Storage*, in: *Catalysis for Sustainable Energy Production*, ed. by P. Barbaro, C. Bianchini, Wiley, 2009, pp. 107–169.

[97] U. Eberle, M. Felderhoff, F. Schüth, *Chemical and Physical Solutions for Hydrogen Storage*, Angew. Chem. Int. Ed., 2009, vol. 48, no. 36, pp. 6608–6630.

[98] J.K. Sun, Q. Xu, *Functional materials derived from open framework templates/precursors: synthesis and applications*, Energy Environ. Sci., 2014, vol. 7, no. 7, pp. 2071–2100.

[99] K.M. Thomas, *Hydrogen adsorption and storage on porous materials*, Catal. Today, 2007, vol. 120, no. 3–4, pp. 389–398.

[100] H.Y. Ammar, H.M. Badran, *Ti deposited C20 and Si20 fullerenes for hydrogen storage application, DFT study*, Int. J. Hydrog. Energy, 2021, vol. 46, no. 27, pp. 14565–14580.

[101] O.M. Korsun, O.N. Kalugin, A.S. Vasenko, O.V. Prezhdo, *Electronic Properties of Carbon Nanotubes Intercalated with Li+ and Mg2+: Effects of Ion Charge and Ion Solvation*, J. Phys. Chem. C, 2016, vol. 120, no. 46, pp. 26514–26521.

[102] M. Li, J. Li, Q. Sun, Y. Jia, *Hydrogen storage in Li and Ti decorated borazine: A first-principles study*, J. Appl. Phys., 2010, vol. 108, no. 6, art. no. 064326.

[103] R. Shahsavari, S. Zhao, *Merger of Energetic Affinity and Optimal Geometry Provides New Class of Boron Nitride Based Sorbents with Unprecedented Hydrogen Storage Capacity*, Small, 2018, vol. 14, no. 15, art. no. 1702863.

[104] F.C. Gennari, F.J. Castro, G. Urretavizcaya, G. Meyer, *Catalytic effect of Ge on hydrogen desorption from MgH2*, J. Alloys Compd., 2002, vol. 334, no. 1–2, pp. 277–284.

[105] B.P. Tarasov, P.V. Fursikov, A.A. Volodin, M.S. Bocharnikov, Y.Ya. Shimkus, A.M. Kashin, V.A. Yartys, S. Chidziva, S. Pasupathi, M.V. Lototskyy, *Metal hydride hydrogen storage and compression systems for energy storage technologies*, Int. J. Hydrog. Energy, 2021, vol. 46, no. 25, pp. 13647–13657.

[106] N.A.A. Rusman, M. Dahari, *A review on the current progress of metal hydrides material for solid-state hydrogen storage applications*, Int. J. Hydrog. Energy, 2016, vol. 41, no. 28, pp. 12108–12126.

[107] M.B. Ley, L.H. Jepsen, Y.S. Lee, Y.W. Cho, J.M. Bellosta von Colbe, M. Dornheim, M. Rokni, J.O. Jensen, M. Sloth, Y. Filinchuk, J.E. Jørgensen, F. Besenbacher, T.R. Jensen, *Complex hydrides for hydrogen storage - New perspectives*, Mater. Today, 2014, vol. 17, no. 3, pp. 122–128.

[108] V.N. Fateev, A.S. Aliyev, *Problems of accumulation and storage of hydrogen*, Chem. Probl., 2018, no. 4(16), pp. 453–483.

[109] P.R. Wilson, R.C. Bowman, J.L. Mora, J.W. Reiter, *Operation of a PEM fuel cell with LaNi4.8Sn0.2 hydride beds*, J. Alloys Compd., 2007, vol. 446–447, pp. 676–680.

[110] C.S. Kim, B.K. Moon, J.H. Park, B.C. Choi, H. J. Seo, *Solvothermal synthesis of nanocrystalline TiO2 in toluene with surfactant*, J. Cryst. Growth, 2003, vol. 257, no. 3–4, pp. 309–315.

[111] J. Zhang, S. Yan, L.P. Yu, X.J. Zhou, T. Zhou, P. Peng, *Enhanced hydrogen storage properties and mechanisms of magnesium hydride modified by transition metal dissolved magnesium oxides*, Int. J. Hydrog. Energy, 2018, vol. 43, no. 48, pp. 21864–21873.

[112] M. Yamauchi, R. Ikeda, H. Kitagawa, M. Takata, *Nanosize effects on hydrogen storage in palladium*, J. Phys. Chem. C, 2008, vol. 112, no. 9, pp. 3294–3299.

[113] K. Wang, G. Wu, H. Cao, H. Li, X. Zhao, *Improved reversible dehydrogenation properties of MgH2 by the synergetic effects of graphene oxide-based porous carbon and TiCl3*, Int. J. Hydrogen Energy, 2018, vol. 43, no. 15, pp. 7440–7446.

[114] S. Guemou, D. Gao, F. Wu, J. Zheng, T. Wei, Z. Yao, D. Shang, L. Zhang, *Enhanced hydrogen storage kinetics of MgH2 by the synergistic effect of Mn3O4/ZrO2 nano-particles*, Dalton Trans., 2023, vol. 52, no. 3, pp. 609–620.

[115] D. Pukazhselvan, N. Nasani, K.S. Sandhya, B. Singh, I. Bdikin, N. Koga, D.P. Fagg, *Role of chemical inter-action between MgH2 and TiO2 additive on the hydro-gen storage behavior of MgH2*, Appl. Surf. Sci., 2017, vol. 420, pp. 740–745.

[116] S.-Y. Lee, J.-H. Lee, Y.-H. Kim, J.-W. Kim, K.-J. Lee, S.-J. Park, *Recent Progress Using Solid-State Materials for Hydrogen Storage: A Short Review*, Processes, 2022, vol. 10, no. 2, art. no. 304.

[117] S.I. Orimo, Y. Nakamori, J.R. Eliseo, A. Züttel, C.M. Jensen, *Complex hydrides for hydrogen storage*, Chem. Rev., 2007, vol. 107, no. 10, pp. 4111–4132.

[118] G. Sandrock, *Panoramic overview of hydrogen storage alloys from a gas reaction point of view*, J. Alloys Compd., 1999, vol. 293, pp. 877–888.

[119] W. Nabgan, B. Nabgan, A.A. Jalil, M. Ikram, I. Hussain, M.B. Bahari, T.V. Tran, M. Alhassan, A.H.K. Owgi, L. Parashuram, A.H. Nordin, F. Medina, *A bibliometric examination and state-of-the-art overview of hydrogen generation from photoelectrochemical water splitting*, Int. J. Hydrog. Energy, 2023, in press.

[120] A.C. Dillon, K.M. Jones, T.A. Bekkedahl, C.H. Kiang, D.S. Bethune, M.J. Heben, *Storage of hydrogen in single-walled carbon nanotubes*, Nature, 1997, vol. 386, no. 6623, pp. 377–379.

[121] O.K. Farha, A.Ö. Yazaydın, I. Eryazici, C.D. Malliakas, B.G. Hauser, M.G. Kanatzidis, S.T. Nguyen, R.Q. Snurr, J.T. Hupp, *De novo synthesis of a metal-organic framework material featuring ultrahigh surface area and gas storage capacities*, Nat. Chem., 2010, vol. 2, no. 11, pp. 944–948.

[122] J.Y. Yong, V.K. Ramachandaramurthy, K.M. Tan, N. Mithulananthan, *A review on the state-of-the-art technologies of electric vehicle, its impacts and prospects*, Renew. Sustain. Energy Rev., 2015, vol. 49, pp. 365–385.

[123] Y. Sun ,G. Zheng, Z.W. She, N, Liu, S. Wang, J. Sun, H.R. Lee, Y. Cui, *Graphite-Encapsulated Li-Metal Hybrid Anodes for High-Capacity Li Batteries*, Chem, 2016, vol. 1, no. 2, pp. 287–297.

[124] S. Yoda, Y. Sakurai, A. Endo, T. Miyata, K. Otake, H. Yanagishita, T. Tsuchiya, *TiO_2-montmorillonite composites via supercritical intercalation*, ChemCom, 2002, vol. 2, no. 14, pp. 1526–1527.

[125] M.Y. Song, Y.J. Kwak, H.S. Shin, S.H. Lee, B.G. Kim, *Improvement of hydrogen-storage properties of MgH_2 by Ni, $LiBH_4$, and Ti addition*, Int. J. Hydrog. Energy, 2013, vol. 38, no. 4, pp. 1910–1917.

[126] M. Tegel, S. Schöne, B. Kieback, L. Röntzsch, *An efficient hydrolysis of MgH_2-based materials*, Int. J. Hydrog. Energy, 2017, vol. 42, no. 4, pp. 2167–2176.

[127] Y.F. Kao, S.K. Chen, J.H. Sheu, J.T. Lin, W.E. Lin, J.W. Yeh, S.J. Lin, T.H. Liou, C.W. Wang, *Hydrogen storage properties of multi-principal-component $CoFeMnTi_xV_yZr_z$ alloys*, Int. J. Hydrog. Energy, 2010, vol. 35, no. 17, pp. 9046–9059.

[128] S.K. Chen, P.H. Lee, H. Lee, H.T. Su, *Hydrogen storage of C14-$Cr_uFe_vMn_wTi_xV_yZr_z$ alloys*, Mater. Chem. Phys., 2018, vol. 210, pp. 336–347.

[129] P. Edalati, R. Floriano, A. Mohammadi, Y. Li, G. Zepon, H.W. Li, K. Edalati, *Reversible room temperature hydrogen storage in high-entropy alloy TiZrCrMnFeNi*, Scr. Mater., 2020, vol. 178, pp. 387–390.

[130] I. Kunce, M. Polanski, J. Bystrzycki, *Structure and hydrogen storage properties of a high entropy ZrTiVCrFeNi alloy synthesized using Laser Engineered Net Shaping (LENS)*, Int. J. Hydrog. Energy, 2013, vol. 38, no. 27, pp. 12180–12189.

[131] V. Zadorozhnyy, B. Sarac, E. Berdonosova, T. Karazehir, A. Lassnig, C. Gammer, M. Zadorozhnyy, S. Ketov, S. Klyamkin, J. Eckert, *Evaluation of hydrogen storage performance of ZrTiVNiCrFe in electrochemical and gas-solid reactions*, Int. J. Hydrog. Energy, 2020, vol. 45, no. 8, pp. 5347–5355.

[132] F. Marques, M. Balcerzak, F. Winkelmann, G. Zepon, M. Felderhoff, *Review and outlook on high-entropy alloys for hydrogen storage*, Energy Environ. Sci., 2021, vol. 14, no. 10, pp. 5191–5227.

[133] G. Zepon, B.H. Silva, C. Zlotea, W.J. Botta, Y. Champion, *Thermodynamic modelling of hydrogen-multicomponent alloy systems: Calculating pressure-composition-temperature diagrams*, Acta Mater., 2021, vol. 215, art. no. 117070.

[134] M. Sahlberg, D. Karlsson, C. Zlotea, U. Jansson, *Superior hydrogen storage in high entropy alloys*, Sci. Rep., 2016, vol. 6, no. 1, art. no. 36770.

[135] D. Karlsson, G. Ek, J. Cedervall, C. Zlotea, K.T. Møller, T.C. Hansen, J. Bednarčík, M. Paskevicius, M.H. Sørby, T.R. Jensen, U. Jansson, M. Sahlberg, *Structure and Hydrogenation Properties of a HfNbTiVZr High-Entropy Alloy*, Inorg. Chem., 2018, vol. 57, no. 4, pp. 2103–2110.

[136] M.M. Nygård, G. Ek, D. Karlsson, M.H. Sørby, M. Sahlberg, B.C. Hauback, *Counting electrons - A new approach to tailor the hydrogen sorption properties of high-entropy alloys*, Acta Mater., 2019, vol. 175, pp. 121–129.

[137] L. Kong, B. Cheng, D. Wan, Y. Xue, *A review on BCC-structured high-entropy alloys for hydrogen storage*, Front. Mater., 2023, vol. 10, art. no. 1135864.

[138] M. Bondesgaard, N.L.N. Broge, A. Mamakhel, M. Bremholm, B.B. Iversen, *General Solvothermal Synthesis Method for Complete Solubility Range Bimetallic and High-Entropy Alloy Nanocatalysts*, Adv. Funct. Mater., 2019, vol. 29, no. 50, art. no. 1905933.

[139] G. Barkhordarian, T. Klassen, R. Bormann, K.-F. Aguey-Zin-Sou, *Hydrogen-Storing Material and Method for Its Manufacture*, US Patent Application Publication, Pub. No. US 2007/0258848 A1, 2007.

Диоксид титана для водородной энергетики: краткий обзор

Н.В. Чиркунова[1,2], N. Islavath[3], М.В. Дорогов[1]

[1] Институт перспективных систем передачи данных Университета ИТМО, Кронверкский пр., д. 49, лит. А,
Санкт-Петербург, 197101, Россия
[2] Научно-исследовательский институт прогрессивных технологий Тольяттинского государственного университета,
ул. Белорусская, 14, 445667, Тольятти, Россия
[3] Analytical Sciences Division, CSIR - Indian Institute of Petroleum, P.O. Mohkampur, Dehradun, 248005, Uttarakhand, India

Аннотация. Наши исследования сосредоточены в основном на решении задач, связанных с производством водорода и его хранением, а также созданием автономных энергетических систем с использованием возобновляемых источников энергии. Технологические решения для зеленой энергетики зависят от разработки новых материалов с заданными свойствами, способных обратимо аккумулировать водород при соответствующих условиях окружающей среды (температура, давление) и от технологических процессов, позволяющих получать молекулярный водород без значительных энергозатрат. Создание материалов с принципиально новыми характеристиками неразрывно связано с получением наноразмерных систем со свойствами, управляемыми на атомно-молекулярном уровне. В обзоре рассмотрены результаты исследований возможностей использования различных наноструктур диоксида титана, известных своими каталитическими свойствами и высокой стабильностью, в различных приложениях водородной энергетики. Большое внимание уделено перспективному направлению твердотельного хранения водорода с использованием гидридных паст и высокоэнтропийных сплавов.

Ключевые слова: хранение водорода; разделение воды; энергетические пасты; высокоэнтропийные сплавы